Affordable Haptic Gloves Beyond the Fingertips

Suyeon Ahn

Thesis submitted to the Faculty of the
Virginia Polytechnic Institute and State University
in partial fulfillment of the requirements for the degree of

Master of Science
in
Mechanical Engineering

Alexander Leonessa, Chair
Alan T. Asbeck
Kaveh A. Hamed
Corina Sandu

September 22, 2023
Blacksburg, Virginia

Keywords: Haptic Gloves, Virtual Reality, Additive Manufacturing

Affordable Haptic Gloves Beyond the Fingertips

Suyeon Ahn

(ABSTRACT)

With the increase in popularity of virtual reality (VR) systems, haptic devices have been garnering interest as means of augmenting users' immersion and experiences in VR. Unfortunately, most commercial gloves available on the market are targeted towards enterprise and research, and are too expensive to be accessible to the average consumer for entertainment. Some efforts have been made by gaming and do-it-yourself (DIY) enthusiasts to develop cheap, accessible haptic gloves, but due to cost limitations, the designs are often simple and only provide feedback at the fingertips. Considering the many types of grasps used by humans to interact with objects, it is evident that haptic gloves must offer feedback to many regions of the hand, such as the palm and lengths of the fingers to provide more realistic feedback. This thesis discusses a novel, affordable design that provides haptic feedback to the intermediate and proximal phalanges of the fingers (index, middle, ring and pinkie) using a ratchet and pawl actuation mechanism.

Affordable Haptic Gloves Beyond the Fingertips

Suyeon Ahn

(GENERAL AUDIENCE ABSTRACT)

Haptics, or simulation of the sense of touch, is already implemented in consumer devices such as smartphones and gaming controllers to augment users' immersive experiences. With the growing popularity of virtual reality, further advancements are being made, particularly in wearable haptic gloves, so users may physically feel the interactions with objects in virtual reality through their hands. Unfortunately, these products are currently inaccessible to the average consumer due to unaffordable pricing. To combat this issue, there have been efforts to develop cheap haptic gloves, but existing designs only provide feedback at the fingertips. Fingertip-only feedback can feel unnatural to users since other areas of the hand are typically also involved when grasping objects.

To address the issue presented by low-cost fingertip haptic gloves, this thesis proposes a design which expands feedback to other areas of the hand while maintaining affordability and accessibility to average consumers.

Acknowledgments

I am incredibly fortunate to be able to say that there were so many people who supported me in this journey that it is difficult to list them all and go into detail about the roles they played. I hope, despite the succinctness, that my feelings will be clearly relayed to everyone; from the bottom of my heart, thank you for your generosity, support, and love.

I would like to acknowledge Dr. Alexander Leonessa as well as the members of the TREC lab, particularly Melanie, Jungsoo, Anchi, Carlo, Christian, Alex, and Zach, for being by my side. Graduate school is a lonely place, but I was surrounded by people who always greeted me with warm smiles and willingness to help. Thank you Mrs. Cathy Hill, as well as my committee members, Dr. Asbeck, Dr. Hamed, and Dr. Sandu for your support during my graduate academic journey. To Thomas, who developed the gloves that this thesis is built on, thank you for your patience and help whenever I needed further insight or clarification. Ananth, I am so grateful your endless patience, kindness, and support.

To Elena, Mac, Patricia, Johanna, Cam, Connie, and Matt, thank you for cherishing me no matter how far apart we are. Your love never fails to find me no matter where I go.

To my grandma who is always waiting so patiently for me in Korea, thank you for waiting and all of the video calls that kept me going. I can't wait to see you soon. To my aunt Haeil, uncle Heesup, and Eric, who are closer to second parents and a brother to me, I am so grateful that we have each other. You never fail to make me smile. Last but not least, thank you Martin for being the sweetest brother who indulges me whenever I need refuge from the hardships of life. To my parents, who always wish for my happiness above all else, and support me without hesitation, thank you for your unshakeable belief in me and affording me the time I need to grow.

Contents

List of Figures

List of Tables

List of Abbreviations

A	Ampere
g	Gram
h	Hour
Hz	Hertz
mAh	Milliampere Hour
min	Minute
mm	Millimeter
ms	Millisecond
Nm	Newton-meter
oz	Ounce
V	Volt
3D	Three-Dimensional
ABS	Acrylonitrile Butadiene Styrene
BOM	Bill of Materials
CAD	Computer Aided Design
CMC	Carpometacarpal

DFA Design for Assembly

DIP Distal Interphalangeal

DIY Do It Yourself

DOF Degree of Freedom

EMF Electromagnetic Field

FDM Fused Deposition Modelling

GPIO General Purpose Input Output

IMU Inertial Measurement Unit

IP Intermediate Phalanx

MCP Metacarpophalangeal

MSB Multi-spool Base

MUX Multiplexer

PCB Printed Circuit Board

pcs Pieces

PIP Proximal Interphalangeal

PLA Polylactic Acid

PP Proximal Phalanx

Qty Quantity

SLA Stereolithography

TMC Trapeziometacarpal

TPU Thermoplastic Polyurethane

USD United States Dollar

VR Virtual Reality

Chapter 1

Introduction

Virtual reality (VR) has been gaining popularity in recent years, especially after being commercialized and applied in gaming and entertainment industries. Consequently, the application of wearable haptic interfaces in entertainment has been increasingly garnering interest as these interfaces are means of augmenting the user's immersion and experience in VR. Although there are several parts of the human body that wearable haptics can be applied to, the most popular region of interest is understandably at the hands, which is one of the most frequently used parts of the human body to manipulate and interact with external objects and the surrounding environment.

Necessary background information, such as the anatomy of the human hand, the types of haptic sensations, and existing haptic glove solutions, are discussed to provide context for the motivations of this thesis. The strengths and weaknesses of existing designs are noted. Finally, a list of design objectives is established.

1.1 Anatomy of the Human Hand

The human hand is comprised of an intricate network of complex joints, bones, muscles, tendons, ligaments, soft tissue, and skin; several kinematic models of the human hand have been developed with varying degrees of freedom (DOFs), such as the Anatomically Correct Testbed (ACT) hand [25], and the Shadow hand [44], but as noted in the review paper

by Bullock et al. [18], a high fidelity model is not always necessary; a simplified model may provide a sufficient framework depending on the application. Conversely, if an oversimplified model is chosen, the resulting glove design may not provide enough DOFs and over-constrain the user into unnatural hand movements, providing an uncomfortable and unpleasant user experience. Since the goal of haptic gloves for VR entertainment applications is to augment the immersive experience, ideally, the gloves should allow the hand to move as naturally as possible, and only provide constraints reflective of the VR environment.

After considering various models, a widely adopted model by Lee and Kunii [37] is chosen for this thesis. Compared to more sensitive applications such as medical robotics, or a prosthetic for a human hand, an affordable haptic glove intended to act as an interface for VR for consumer entertainment does not require a very advanced model fidelity. As mentioned before, it can be unnecessary and even undesirable to adopt a highly complex model as the increased complexity will impact the glove design, and in return, its cost. It is important to choose an appropriate model which will not over-simplify the hand to the extent that the user experience is severely impacted, but not excessively intricate that the glove design becomes too expensive or complicated for consumer use.

As shown in Figure 1.1, there are three bones in the index, middle, ring, and pinkie (little) fingers, called the distal, intermediate (also referred to as middle), and proximal phalanges. The bones in the palm of the hand are called the metacarpal bones, and the wrist is comprised of eight small bones called the carpal bones. The thumb differs from the other four digits as it only has two phalanges and does not have an intermediate phalanx. In Lee and Kunii's model, the joints between the distal and intermediate phalanges, called the distal interphalangeal (DIP) joints, and the joints between the middle and proximal phalanges, called the proximal interphalangeal (PIP) joints, each have 1 DOF for flexion and extension (curling and straightening) of the fingers. The knuckles, which are the joints between the

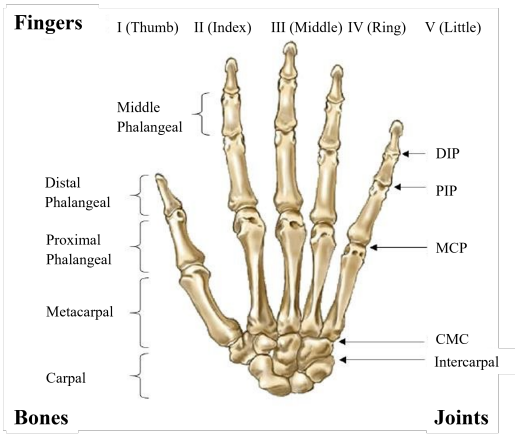

(a) Bones and joints of a human hand [17]

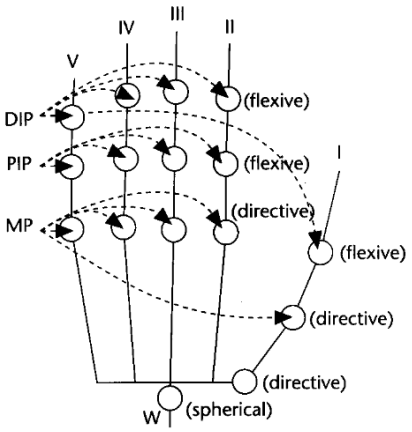

(b) Hand Model by Lee and Kunii [37]. Flexive = 1 DOF, directive = 2 DOFs, and spherical = 3 DOFs

Figure 1.1: The human hand and kinematic model by Lee and Kunii [37]

proximal phalanges and the metacarpals, are called the metacarpophalangeal (MCP) joints and each have 2 DOFs, one which is responsible for flexion and extension like the DIP and PIP, and one for abduction and adduction. The thumb has an interphalangeal joint between its distal and proximal phalanx, but does not have a PIP joint. The joint between the metacarpal and carpal bones is called the carpometacarpal (CMC) joint and is present for each digit. The CMC joints for the index and middle fingers are joined in a way that renders them nearly immobile; these joints primarily provide rigidity and structure to the hand. The ring and pinkie CMCs are constrained such that they offer limited motion. Functionally, these CMCs provide indirect movements that support the agility of the hand, but are not used to produce direct movements of their own. Thus, these joints are not considered to provide DOFs in the simplified model of the hand. The thumb CMC, which is also known as the trapeziometacarpal (TMC) joint, is represented by 2 DOFs. Lastly, the wrist has 6 degrees of freedom, three for rotational motion, and three for translational. It should be noted that the wrist does not possess the mechanism to twist on its own- the wrist twists with the forearm, which is responsible for the actuation of this degree of freedom. However,

since this degree of freedom is necessary to determine the pose of the hand, Lee and Kunii's model incorporates this degree of freedom at the wrist. Therefore, the human hand is modelled through 27 DOFs. The wrist is modelled as a single joint, while the metacarpals and phalanges are modelled as simple linkages.

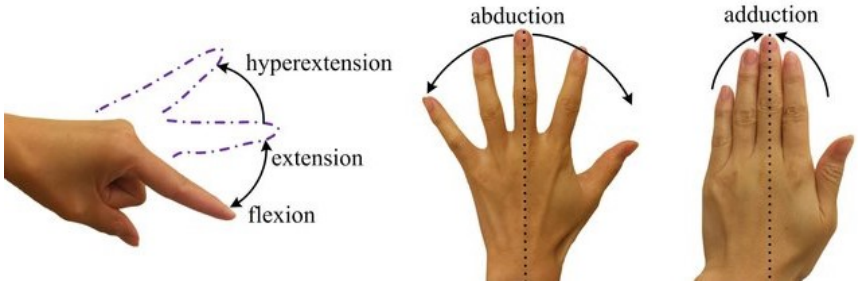

Figure 1.2: Finger motions [53]

In Lee and Kunii's work, it is assumed that the DIP joint in each finger is dependent on the respective PIP joint and cannot be moved independently. Although this assumption does not hold for all scenarios, it holds true in most situations when the hand is not constrained unnaturally. An approximation of $\theta_{\text{DIP}} = 2/3 * \theta_{\text{PIP}}$ is used, but a more recent study by Hrabia et al. [33] shows that the relationship between the DIP and PIP joints are better modelled by $\theta_{\text{DIP}} = 0.88 * \theta_{\text{PIP}}$. This thesis will adopt the latter relation, thus reducing the number of independent DOFs by four.

1.2 Haptics and the Human Grasp

Thousands of sensory receptors within the skin, muscles, and tendons are responsible for the sense of touch. Huang et al. [34] categorizes haptic feedback as either kinesthetic or tactile, describing kinesthetic haptics as forces and torques that are felt through the receptors in muscles and tendons, while tactile haptics are sensations such as vibration, temperature, pressure, and texture, felt through various types of receptors in the skin.

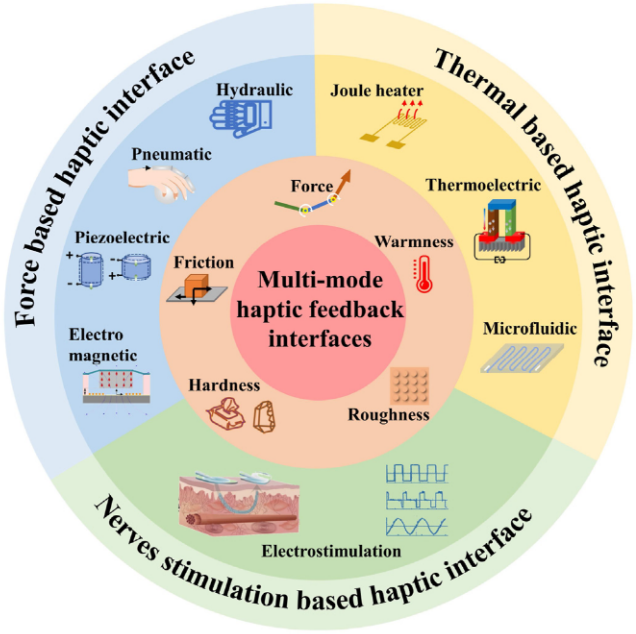

Figure 1.3: Haptic feedback modes and means [34]

As shown in Figure 1.3, Huang et al. [34] further summarizes haptic sensations into five modes: temperature, force, friction, hardness, and roughness, and lists various mechanisms that can be used to achieve one or more of these sensations.

Haptic simulation of temperature is difficult due to the constraints of physics; in VR, it is possible for a user to rapidly alternate between touching "hot" and "cold" objects, but to simulate this, the haptic interface must rapidly change to the appropriate temperature of the object being contacted at a given time. Depending on the type of material and method used, it may not be physically possible for the interface to change temperatures at the pace set by the user, since material properties and thermodynamic laws govern the amount of energy and time required to change the temperature of an object. Additionally, many thermally conductive materials capable of dissipating heat quickly enough for haptic applications have poor elasticity and other material properties that limit wearability. As a result, thermal haptic glove interfaces are mostly found in research and are rarely commercial.

Vibrational haptics is one of the most common forms of tactile haptic feedback and can be found in gaming controllers, cellular devices, wearable haptics, and other commercial products. Vibration can be used to simulate textures; as the skin travels across a surface, the vibrations caused create a sense of roughness or smoothness. However, this type of feedback is unable to simulate other physical properties, such as the mass, elasticity, or dimension, of an object. For example, a haptic glove with vibrational haptic feedback at the fingers will not be able to simulate the normal forces that occur when the user grabs an object. The actuators responsible for creating this type of haptic feedback are often compact and lightweight, which make them easy to implement at a wide variety of locations.

Force haptics is also a common form of feedback. Unlike vibrational haptics which cannot simulate mass, elasticity, or dimension, force feedback provides kinesthetic simulation and is able to simulate the normal forces that the user should experience when interacting with an object. Force feedback haptic gloves are often categorized into active or passive systems; active force feedback can apply varying amounts of force to the user's hand independent of the user, which allows for simulation of elasticity, hardness, and mass. For example, non-rigid objects will often provide varying amounts of normal force depending on the displacement of the object's material. A passive force feedback system can only provide a force proportional to the force being applied by the user, or the force that can be tolerated by the material of the glove, whichever is lesser. This type of feedback is only able to simulate rigid objects, and cannot simulate the mass. Compared to vibrational haptics, force haptics often require larger, cumbersome systems as more powerful actuators are required. This also limits the regions in which force feedback can be applied; the most common region of application for this type of feedback is at the fingertips.

However, humans demonstrate complex grasping motions that often utilize many areas of the hand beyond the fingertips. Feix et al. [29] classifies grasping motions into 33 types

(see Figure 1.4) and reports the frequency of the grasps that occurred in a study of two housekeepers and two machinists. The grasp that occurred with the highest frequency is #3, the medium wrap, which clearly employs the full lengths of the fingers as well as the palm.

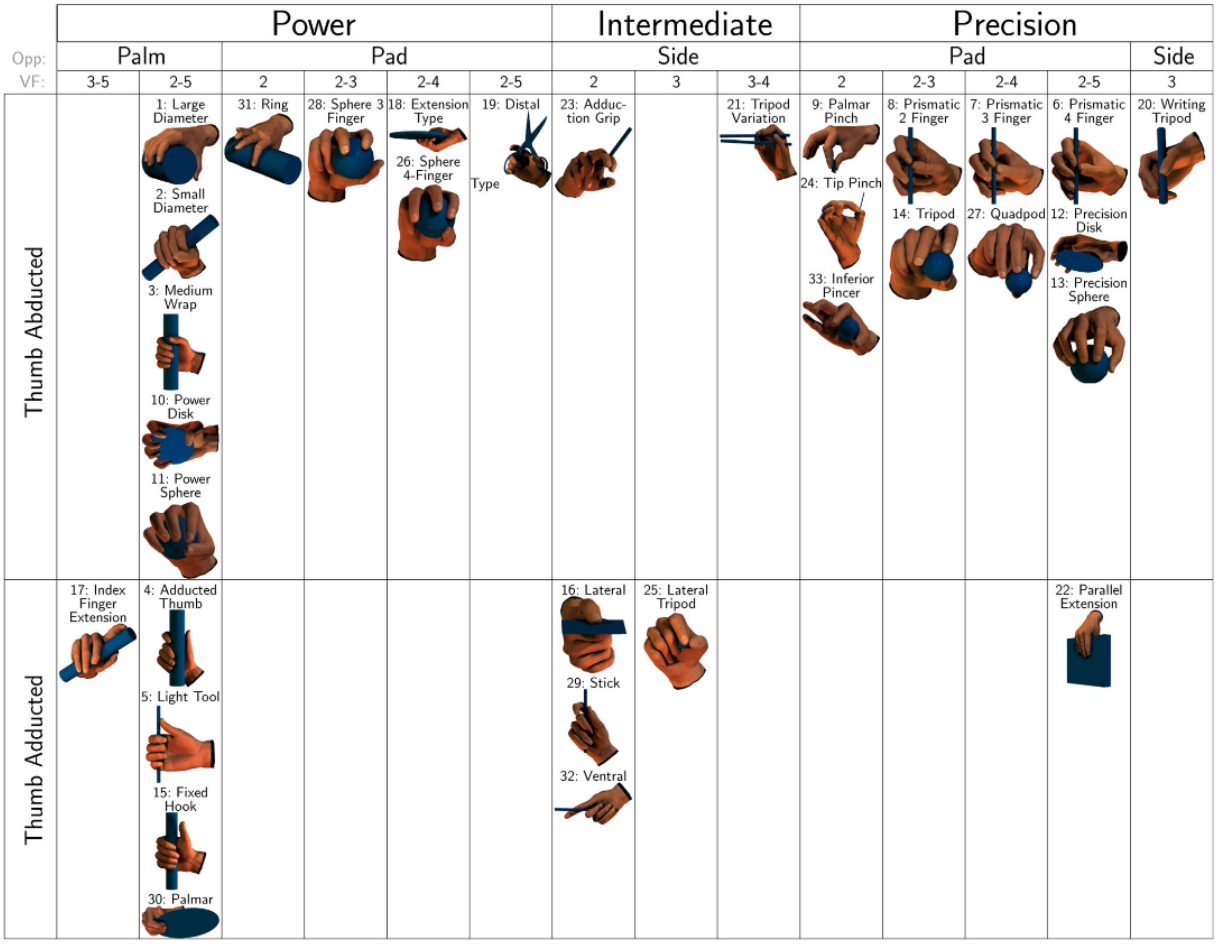

Figure 1.4: Grasp types categorized by Feix et al. [29]

1.3 Haptic Gloves in Literature and the Commercial Market

The haptic gloves that are currently available can be divided into two categories: gloves that have been developed for research and innovation (non-commercial), and gloves that are being produced commercially. The recent review paper by Caeiro-Rodríguez et al. [19] provides a comprehensive list of gloves that were commercially available as of 2021, from papers published between 2015 and 2021. The compiled list of gloves are characterized by several factors such as cost, fields of application, finger tracking, haptic feedback technologies used, etc. The paper provides the approximate cost of 24 gloves, which may vary depending on the configuration and accessories included; the paper notes that "*the prices are generally above €1000,*" which would have been approximately equivalent to $1182 USD at the time, using the average 2021 conversion rate of $1 USD to € 0.846 [47]. Of the 24 gloves, only two are priced below $995 USD, and the cheapest listed glove is the CaptoGlove with a pricing of $315 USD. Although many of the gloves in the review paper are listed as applicable to the video game industry, the pricing of the majority of these gloves are too expensive for individual consumers to purchase. Most of the gloves listed in the review paper utilize inertial measurement units (IMUs) and/or bend sensors to determine hand pose. Only three of the listed gloves are reported to provide kinesthetic feedback, while nine of the gloves provide tactile feedback. The cheapest listed kinesthetic feedback glove priced at €2999, equivalent to $3544.92 USD, while the cheapest tactile feedback glove is priced at €500, or $591.02 USD. Since the publication of the paper, additional commercial gloves have become available by companies such as HaptX [32] and Teslasuit [49], but most of these gloves also cost several thousands to tens of thousands of dollars, and are currently primarily targeted for enterprise and scientific use, not consumer entertainment. A more recent commercial haptic glove

called the TactGlove by bHaptics, which costs $299, has a more affordable pricing than the cheapest listed glove in the review paper but only provides tactile feedback at the fingertips and wrist [30].

Figure 1.5: Commercially available haptic gloves reviewed by Caeiro-Rodríguez et al. [19]

Many non-commercial gloves are inaccessible to the average consumer due to the implementation of niche technology or because the designs are not released for public use. However, there have been efforts within research, do-it-yourself (DIY), and gaming communities to develop open source, low-cost haptic glove designs to provide solutions that address the demand for accessible haptic gloves for VR entertainment. Especially as additive manufacturing technologies, such as fused deposition modelling (FDM) and stereolithography (SLA)

3D printers, have become accessible to consumers, it has become possible for consumers to overcome traditional manufacturing hurdles and develop products relatively inexpensively in-house. One popular open source haptic gloves is called the LucidGloves [24], which uses 3D printed parts, cheap, lightweight servos, and cheap potentiometers to provide rudimentary passive force haptic feedback at the fingertips. Other examples include Open Glove, which provides customizable vibrotactile feedback to different areas of the hand. Unfortunately, these designs often sacrifice user experience to simplify the glove design as much as possible to be economical and accessible to hobbyists who may not have extensive experience in building electro-mechanical assemblies. Fingertip-only feedback provides an unnatural user experience because human grasping motions often employ many parts of the hand, not just the fingertips, as discussed in Section 1.2. There is a notable lack of open-source, affordable designs that provide kinesthetic feedback to areas of the hand beyond the fingertips.

1.4 Design Objectives

As discussed in the previous section, many of the existing solutions for haptic gloves are either too expensive to be applied to the consumer entertainment market, or features limited and over-simplified haptics, which has a detrimental and unnatural impact on the user experience.

The objective of this thesis is to propose a low-cost, accessible haptic glove design which provides force feedback to areas of the hand beyond the fingertips, thus, creating a more realistic user experience in VR. Most low-cost haptic gloves provide feedback at the fingertips, but this limited range of feedback is often incongruous with natural human grasping motion, in which the full lengths of the fingers, as well as the palm are often used to contact the object. Fingertip-only force feedback mechanisms give the illusion that the user is always pinching objects in VR. Providing haptic feedback at the intermediate and proximal phalanges, as

well as the palm is crucial for providing a more natural and intuitive user experience.

There are existing designs in research proposing haptic feedback for the palms, such as the works by Dragusanu et al. [26] and Son and Park [48], so this thesis will focus on haptic feedback to the intermediate and proximal phalanges of the fingers. Specifically, the palm side of the intermediate and proximal phalanges will be targeted, because these areas are more frequently engaged than the back (dorsal) side of the hand when humans interact with their surrounding environments. The thumb is omitted from the scope of this thesis as it is anatomically and physiologically different from the other digits. In total, eight regions of the fingers will be actuated.

Figure 1.6: Areas of interest for haptic feedback [28]

The proposed design in this thesis aims to satisfy the following goals:

1. Consumer friendly price

   The cost of the gloves should be accessible to average consumers, and not exceed the price of commercially available gloves. The survey and market research completed by Aujas [16] concluded that surveyors felt that £50-100 (equivalent to $68.79 to $137.57

USD at the time, using the average conversion rate for that year of £1 to $1.3757 USD [50]) is a reasonable price range.

2. Easy to assemble

   The assembly of the glove should not be exceedingly difficult, and should be easy to assemble for average consumers.

3. Lightweight and compact

   The glove must not be so heavy or unwieldy that it becomes unusable.

4. Ergonomic

   The glove should be comfortable for the user to set up, wear and use.

5. No noticeable latency

   The latency standard for computer-human interfaces is $200ms$ according to the findings from Miller [41]. The latency of the system should not exceed this threshold, so that the computed responses will seem instantaneous to the user.

6. Portability

   Ideally, the glove should be wireless so that there are no constraints placed on the user's movement. However, if a wireless design is not possible, the grounding method should be chosen such that the impacts to the user are minimized.

7. Compatible with most systems

   As there are many VR systems available, the glove should be universally compatible and not specific to one system.

8. Realistic haptic feedback to the eight target areas

   In real life, the feedback to the intermediate and proximal phalanges are mostly independent. For example, when fingers are wrapped around a water bottle, the proximal

phalanges will contact the walls of the bottle and be constrained before the intermediate phalanges contact the bottle and become constrained. The glove should provide feedback that mimics reality for an immersive experience.

Chapter 2

Haptic Glove Mechanical Design

2.1 Base Glove Selection

To provide appropriate haptic feedback to the hand when the user interacts with an object in VR, the following information must be known: the position and orientation of the object relative to the hand, the pose of the hand, and the points of contact between the hand and the object. The collision detection between an object and the hand are determined in software, but the pose, position and orientation of the hand must be obtained through the glove and its sensors.

There already exist solutions for capturing hand pose and orientation, so it is unnecessary to design a novel mechanism as long as an existing solution can meet the requirements. The various designs that are considered will be discussed, as well as the reasoning that ultimately led to the selection of one design over the rest.

When looking for a base glove design, it is crucial that the design is able to fully capture the DOFs of interest, in accordance with Lee and Kunii's hand model. Since this thesis focuses on haptic feedback to the intermediate and proximal phalanges of the four fingers, the full 27 DOFs can be reduced by eliminating the 5 DOFs from the thumb. In addition, most VR entertainment systems, such as the HTC VIVE, Meta Quest, and PlayStation VR, utilize controllers which interface with either built-in cameras in the headsets or external trackers,

such as the base stations for HTC VIVE, to track the hand position and orientation. Since these systems already track the 6 DOFs at the wrist, it is also not necessary for the base glove design to be able to capture and provide this information. Lastly, Lee and Kunii's hand model assumes that the DIP joints are dependent on the PIP joints, so it is not required for the base glove to have DIP joints tracking capabilities. Thus, the total number of DOFs of interest is 12, which is comprised of 1 DOF at each PIP joint, and the 2 DOFs at each MCP joint. Although this is the set of strictly required DOFs, a glove that can measure the other DOFs is be preferred as it would provide greater opportunities for future work and development.

Hand tracking is possible without mounting hardware on the hands. There exist VR systems that utilize the cameras in headsets to track the wearer's hands, which allows for the most natural user experience, as there are no loads or constraints on the hands. Although this approach requires no cost or hardware for the base glove, making it the lightest design, the headset or alternative camera hardware becomes indispensable; for VR systems that do not provide hand tracking, accessories can be purchased to provide these capabilities, such as the Leap Motion Controller by Ultraleap [51], which costs $139. Additionally, the haptic feedback mechanism must be designed from scratch since there is no pre-existing hardware that can be used as a foundation. Although the haptic feedback mechanism would not be constrained by pre-existing hardware and can be optimized, the design would likely be costly, as external hardware must be purchased to make the system universally compatible.

As presented in the review of existing commercial gloves by Caeiro-Rodríguez et al. [19], most commercial gloves rely on IMUs or bend sensors to measure the pose of the fingers. Some gloves that utilize these technologies are considered, such as the the MiMu glove [38], which features eight bend sensors; one each in the thumb and pinkie, and two each for the index, middle and ring fingers. An IMU mounted near the wrist of is utilized to measure the

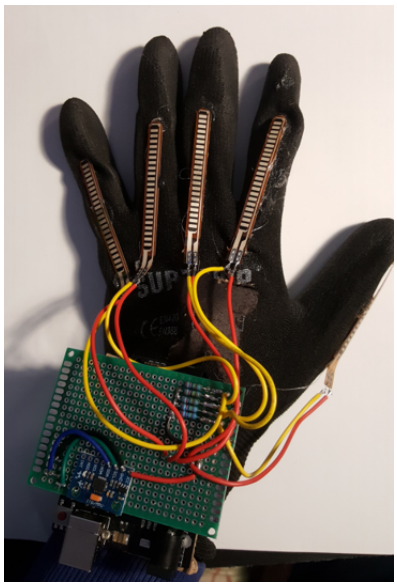

(a) Bend sensor glove by Ng [42]

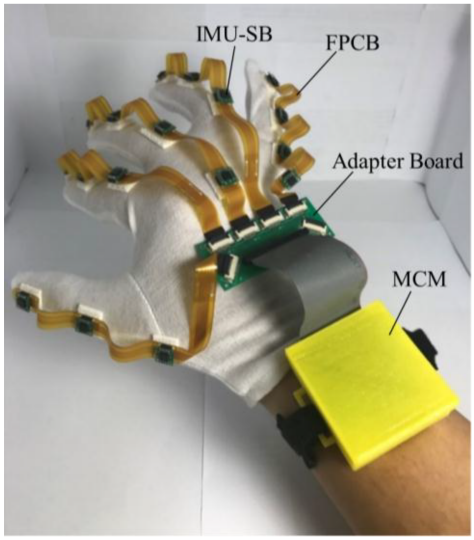

(b) IMU glove by Lin et al. [39]

Figure 2.1: Gloves measuring hand pose using IMUs and bend sensors

orientation of the hand, or the 3 rotational DOFs of the wrist. However, this glove is unable to capture the minimum required DOFs, and its price of $3430 USD [20], which is in the range of many commercial haptic gloves, makes it an unjustifiable choice. Similarly, another commercial glove that uses IMUs and electromagnetic field (EMF) sensors to capture hand pose, called the Smartgloves [45], is priced $1495 USD, making it too expensive to be used as a base glove. Other considerations include the flex sensor glove by Ng [42], which utilizes bend sensors on each finger. However, bend sensors are more expensive than IMUs, and can only measure the overall bend angle between the two ends of the sensor. Therefore, the design proposed by Ng [42], which only features one bend sensor per finger, would not be able to measure all of the required DOFs. The flex sensor glove design can be modified to have multiple flex sensors in each finger to measure the required DOFs, but flex sensors that are short enough for this application are not commercially available. A glove that utilizes IMUs proposed by Lin et al. [39] is also considered. This glove features 18 IMUs mounted on flexible printed circuit boards (PCBs) that would be able to capture all of the required

DOFs, making it a possible candidate to be used as the base glove design. Although the design is light, flexible PCBs are expensive, and failure through fatigue becomes a large concern since the PCBs will undergo repeated bending due to movement of the hands.

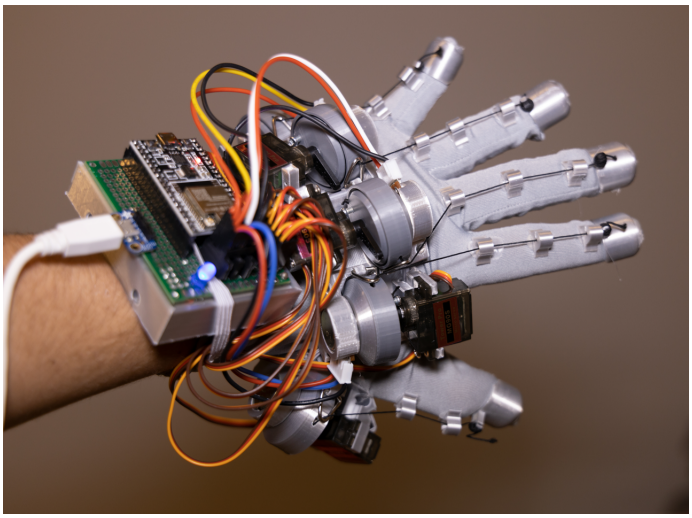

Figure 2.2: LucidGloves [23]

As mentioned in Section 1.3, LucidGloves is a popular open-source haptic glove design for VR entertainment applications. Its cost-effective and relatively simple design has been well-received by DIY and gaming enthusiasts. Unfortunately, the LucidGloves design is difficult to use as a base for expanding haptic feedback because the system is unable to measure the individual angles of the joints in the finger. The design features potentiometers which are each connected to a spring-loaded spool. One end of a non-elastic string is connected and wound about the spool, while the other end is fixed to the end of a finger. As each finger curls forward, the string is unwound from the spool, which turns the connected potentiometer. The potentiometer is connected to a microcontroller which detects the resultant change in resistance and provides the data to the computer, where the data is used, along with several simplifications and assumptions, to approximate the flexion of the DIP, PIP and MCP joints. Inverse kinematics cannot be used to find an accurate, unique solution to this problem despite known angle limitations of finger joints because the position of the fingertip is not known, and

cannot be determined by the displacement of string from the spool. Therefore, it would be impossible to determine the actual pose of the user's hand and whether the intermediate or proximal phalanges would contact an object in VR. Therefore, LucidGloves is an unsuitable design to be used as a foundation for this thesis.

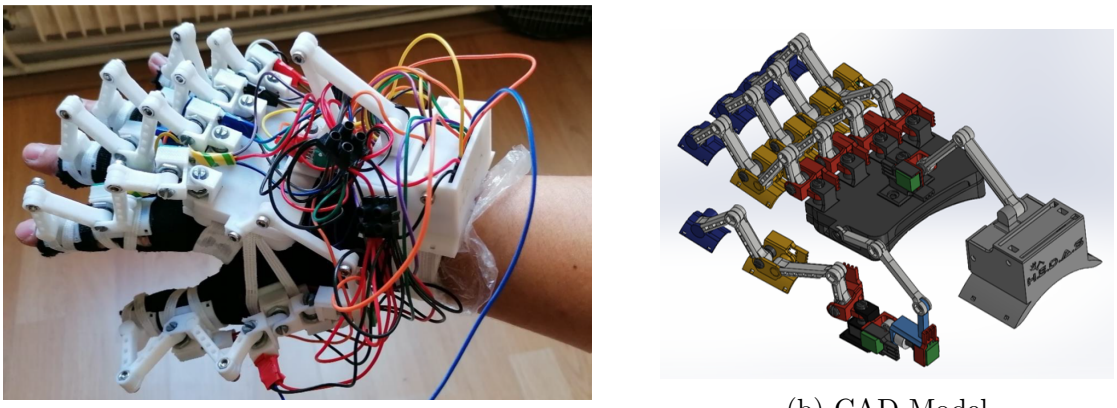

(a) Prototype

(b) CAD Model

Figure 2.3: HEDAS [16]

Another open-source project called HEDAS [16] is a 3D printed glove that does not have any haptic feedback capabilities, but is able to measure 19 DOFs. Although the model used in HEDAS is not identical to Lee and Kunii's model, the differences occur at the thumb and wrist joints; the wrist is considered to have 2 DOFs by only considering angular motions, not linear, and by omitting twist, and the TMC joint is considered to have 2 DOFs. The phalangeal joints are modelled identically, so the discrepancies do not pose any problems. Furthermore, HEDAS provides a flat platform on the back of the hand where a haptic mechanism can be mounted, and the rigid 3D printed links can be used as interfaces through which haptic feedback can be provided. Potentiometers, although less reliable than IMUs, are cheaper. Therefore, HEDAS provides an excellent base glove design and is chosen as the foundation for this thesis.

Figure 2.4a displays the HEDAS finger assembly used for all fingers. The dark blue and

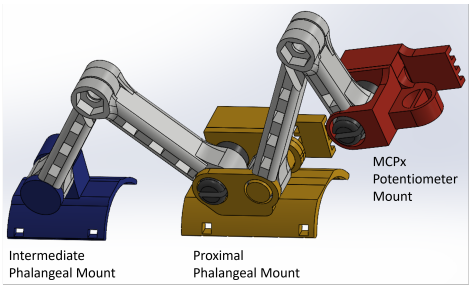

(a) HEDAS Finger Assembly

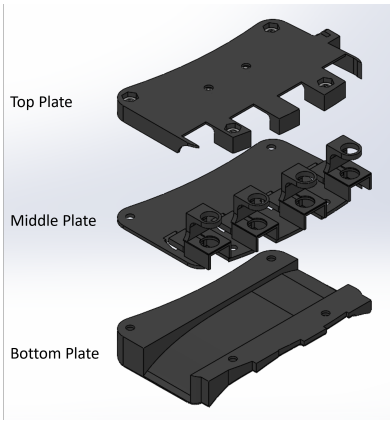

(b) HEDAS Plate Assembly (Exploded View)

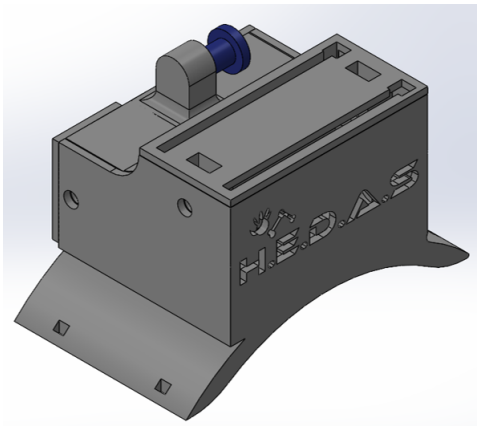

(c) HEDAS Electronics Box

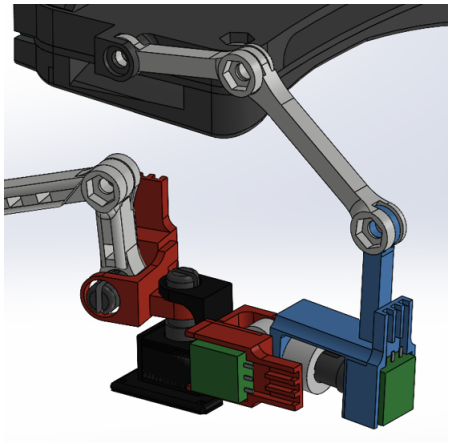

(d) HEDAS Thumb MCP and CMC Assembly

Figure 2.4: HEDAS Design Features [16]

yellow components are used to mount to the dorsal side of the intermediate and proximal phalanges. The yellow and red components are used to mount potentiometers responsible for measuring the PIP and the flexion/extension DOF at the MCP joints (referred to as MCPx by Aujas), respectively. The dark grey plate assembly is comprised of three parts (see Figure 2.4b) called the top, middle and bottom plates. The top plate provides a mounting surface for the potentiometers that measure the DOFs of the wrist, while the middle plate has mounting features for potentiometers that measure the adduction/abduction DOF at the MCP joints (referred to as MCPz by Aujas) of the index, middle, ring, and pinkie fingers.

The bottom plate is a mounting interface between the glove and the dorsal side of the hand. The mounting components are connected using the light grey linkages, which have varying lengths. The electronics box (see Figure 2.4c), which is designed to be mounted close to the base of the wrist on the forearm, is used to measure the wrist DOFs, as well as store a multiplexer (MUX) and microcontroller. The thumb also utilizes the finger assembly, but because the anatomy of the thumb differs from the other fingers, additional potentiometer mounts are introduced. The dark blue component of the finger assembly mounts to the thumb's distal phalanx, the yellow component mounts to the proximal phalanx, and the black MCP potentiometer mount (next to the red MCP mount on the left in Figure 2.4d) is attached to the thumb's metacarpal. The extra red potentiometer mount as well as the light blue mount to the right in Figure 2.4d are responsible for measuring the thumb's CMC DOFs.

2.2 Haptic Mechanism Design

Since the goal is to actuate the eight areas of the hand independently, it is expected that eight actuators will be used. A gear shifting mechanism is considered as a means to reduce the number of required actuators, thereby reducing the cost and, potentially, the weight of the mechanism. With a gear shifting mechanism, the only two actuators would be required- one to shift between the actuation transmissions for the eight regions of the finger, and one actuator to provide the force feedback. Unfortunately, this would make the eight feedback regions dependent, as only one region could be actuated at a given time. If the shifting mechanism is fast enough, it may be possible to actuate the various regions in sequence quickly enough that it seems instantaneous to the user, but due to the complexities involved in gear shifting, the latency would likely be noticeable.

Due to the constraints of weight, size, as well as cost, an active haptic feedback mechanism design is quickly dismissed. Active haptic mechanisms require a greater level of design complexity than passive haptic feedback designs, since the amount of force being output by the actuator must be monitored and controlled at all times. Additionally, compared to passive feedback systems, more powerful actuation is required for active feedback, which typically results in larger, heavier, more expensive actuators. The trade off between output force and space poses many challenges; direct drive, though it provides the least amount of force transmission loss, is unfeasible due to space constraints. A high speed, low torque actuator can be utilized with a step down drive, but this option also requires substantial space for the step down gear train. Although small, powerful motors can be purchased, they are too expensive to be considered accessible to consumers. Additionally, these powerful actuators would add significant weight to the design. Although active actuation (which utilizes an actuator to introduce energy into the system) would allow the user to interact with a greater variety of objects, such as animate or elastic objects, passive actuation (which is only able to remove energy from a system, such as a brake [14]) is sufficient for interactions with rigid, inanimate objects. For these reasons, a passive haptic feedback mechanism design is pursued.

For the passive feedback design, the weight loaded onto the fingers should be minimized, since fingers can not handle as much load compared to the back of the hand. The majority of the weight should be offloaded to either the back of the hand or the upper arm of the user, and rely on lightweight, compact transmissions to apply actuation at the fingers. Furthermore, it is expected that the actuators used will be small, lightweight, and not very powerful, so the torque used to stop the flexion of the fingers should not be provided directly from the actuator if possible.

Similar to the haptic mechanism of the LucidGloves, a passive haptic feedback mechanism

only for the palm side of the hand requires a means of preventing flexion when necessary, while always allowing extension of the fingers. After assessing the HEDAS glove design, it is recognized that if the linkages of the HEDAS glove, which are connected to the fingers, are restricted from rotating forward, then the connected phalanges will also be prevented from further flexion. Utilizing the linkages (as shown in Figure 2.4a), which are essential to the HEDAS design, is ideal as it uses an existing feature, thus minimizing the weight that is added due to the haptic mechanism. Strings can be used to connect to the linkages to the haptic mechanism, thereby allowing offloading of the mechanism to the back of the hand.

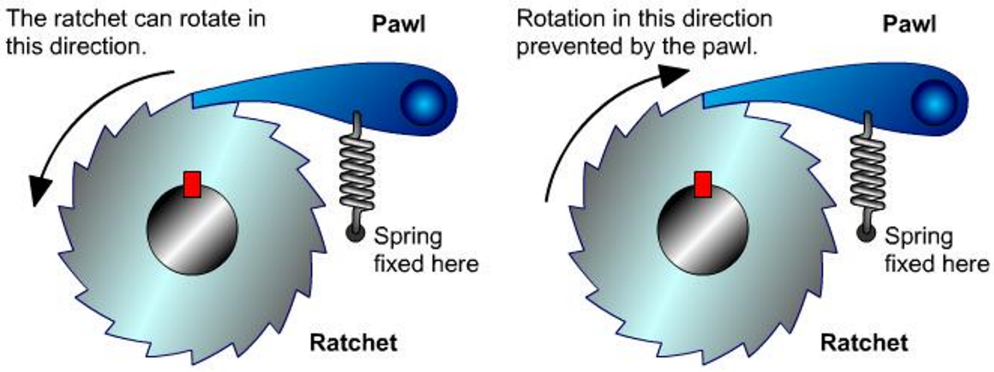

Figure 2.5: Ratchet and Pawl Mechanism [40]

There are several designs that are considered for the haptic mechanism, such as the mechanism used by LucidGloves, a micro-clutch, a one-way clutch bearing, and a ratchet and pawl mechanism (shown in Figure 2.5). A one-way clutch bearing relies on wedging a roller between the inner and outer races of the bearing to achieve free rotation in one direction while restricting rotation in the opposite direction. Unfortunately, rotation is always restricted in one direction, which does not meet the requirements. There are several varieties of micro-clutches available commercially, but it is difficult to find a clutch that has a small enough footprint to be able to mount eight of them. The LucidGloves mechanism is also too large to be able to fit eight mechanisms on the back of the hand because it requires micro

servos to be aligned co-axially with the spring-loaded spool. A ratchet and pawl mechanism is stackable and requires minimal thickness, so it is the most promising mechanism that would likely be able to fit on the back of the hand.

Figure 2.6: Badge Reel Anatomy [27]

Applying the ratchet and pawl concept, the ratchet gear doubles as a spool to which the other end of the string connected to the linkages is fixed and wound about. The ratchet gear also needs to be spring loaded to ensure that tension is always kept in the string, to ensure that the force from the haptic mechanism is properly transmitted to the linkage. Taking inspiration from the LucidGloves design, spring loaded spools are sourced from off the shelf (OTS) badge reels. Rather than having each component sourced independently, the outer housing of the badge reels can be removed to extract the pre-assembled spool, string, and spring required for the ratchet mechanism. Additionally, these parts are sold in bulk inexpensively by online businesses, thus saving assembly time as well as cost.

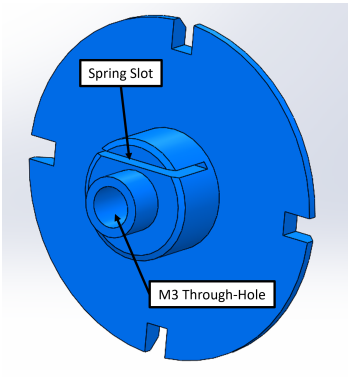

(a) Front view of the shaft

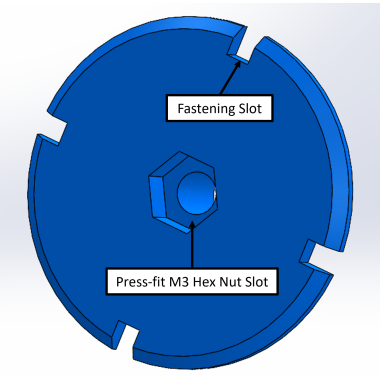

(b) Rear view of the shaft

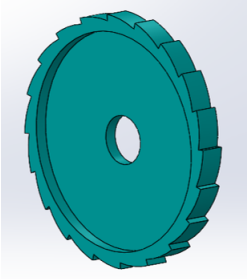

(c) Gear

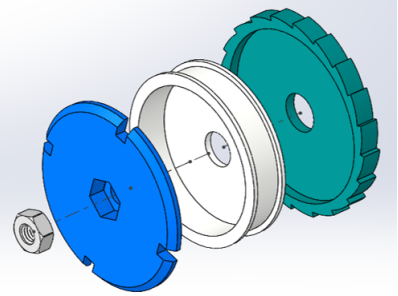

(d) Exploded view of the spool assembly

Figure 2.7: Components of the Spool Assembly

The spool extracted from the badge reel must be mounted on a fixed shaft, to which one end of the spring must be attached. To achieve this, an M3 bolt is used as a fixed shaft, because the threads would ensure that the bolt will not rotate. Unfortunately, the bolt poses two challenges. Firstly, because the wall of the spool is so thin, and the threads of the bolt do not provide a smooth cylindrical surface, the rod will not allow the spool to rotate smoothly. Secondly, there is no means of attaching the end of the spring to the bolt. To address these problems, a shaft part is designed as the interface between the bolt, spool, and spring. The part features a recess for an M3 hex nut, which ensures that the shaft will be fixed, as well as a slot for the end of the spring to attach to. When the spool is rotated and the spring is wound, although the majority of the potential energy in the spring is converted to rotational energy, some of the energy is converted axially and the spring may jump out of the spool.

To prevent this, the shaft also incorporates a cover to retain the spring inside of the spool, as well as limit the amount of axial force. Taking design for assembly (DFA) into consideration, four slots are provided around the perimeter of the shaft as leverage points that can be used to fasten the shaft.

To incorporate gear teeth to the spool, a gear part featuring a recess for the spool to press fit into is designed. The press fit allows for easy assembly, and also ensures that the gear cannot rotate independently of the spool. The number of gear teeth is an important design consideration as it determines the resolution of the haptic feedback mechanism. A ratchet can only be engaged and stopped by the pawl from further rotation at the flat faces of the gear teeth. Therefore, if the pawl is positioned between two stopping points, the string connected to the spool can be pulled until the gear is rotated to the next occurring engage point before braking. The maximum length of string that can be unwound from the spool before braking is guaranteed by the resolution of the haptic mechanism. Ideally, the number of gear teeth would be maximized to minimize the amount of travel needed to ensure braking, but a greater number of gear teeth would result in smaller teeth, which would reduce the amount of force that can be handled by the mechanism. Additionally, if the teeth are too small, the pawl may not be able to engage properly, or the features may exceed the printing capabilities of FDM 3D printers. The resolution of the mechanism (r) can be determined by the following relationship with the diameter of portion of the spool that the string wraps around (d_{spool}) and the number of gear teeth (N_{gear})

$$r = \frac{d_{\text{spool}} * \pi}{N_{\text{gear}}}. \tag{2.1}$$

The gear tooth dimensions are defined by the tip diameter (d_{tip}), the root diameter (d_{root}), and the number of teeth. To ensure that the size of the mechanism is minimized, the tip

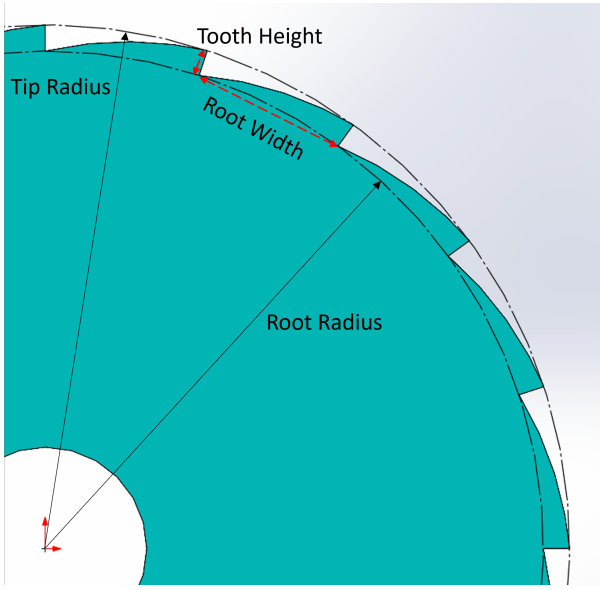

Figure 2.8: Gear Dimensions

diameter is chosen to be $30mm$, which is only $4mm$ larger than the outer diameter of the spool. The root diameter is defined to be $28.5mm$. The width of the root, which is the length of the chord that connects the roots of two adjacent gear teeth (l_{root}) is

$$l_{\text{root}} = d_{\text{root}} * \sin \frac{180^\circ}{N_{\text{gear}}}. \tag{2.2}$$

The height of the tooth (h_{tooth}) is constant, since it is simply the difference between tip and root diameters divided in half

$$h_{\text{tooth}} = \frac{d_{\text{tip}} - d_{\text{root}}}{2}. \tag{2.3}$$

Therefore, the tooth height is $0.75mm$. The diameter of the portion of the spool that the string wraps around is measured to be $24.35mm$. The relationship between the resolution of the haptic mechanism, the gear tooth root width, and the number of gear teeth is shown in Figure 2.9. As the number of gear teeth increases, the improvement in resolution becomes

smaller, until it becomes negligible and the resolution becomes nearly constant. Similarly, the decrease in root width becomes smaller until it becomes negligible.

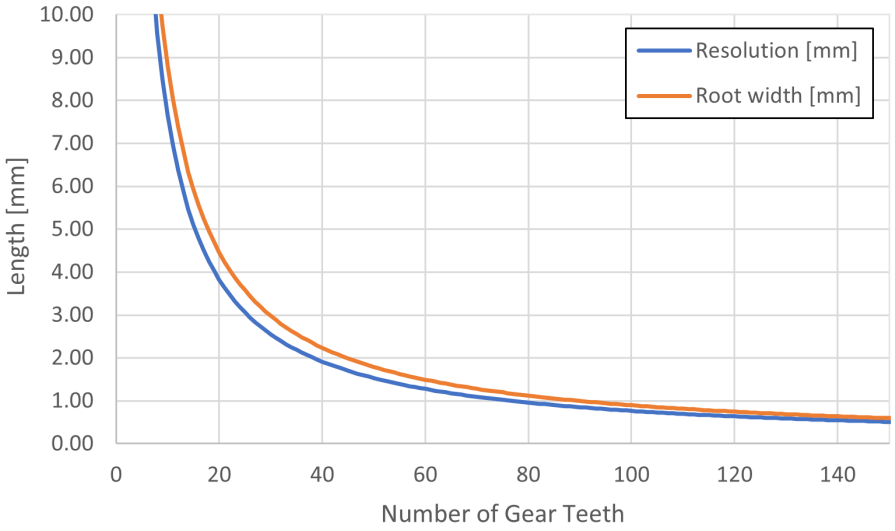

Figure 2.9: Impacts of the Number of Gear Teeth

Based on the above relations, the number of gear teeth is chosen to be 20, which results in a $4.5mm$ root width, ensuring that the part can be 3D printed without issues, and a resolution of $3.8mm$.

The profile of the ratchet gear teeth is used to design the mating pawl. The example ratchet and pawl mechanism shown Figure 2.5 has the pawl mounted above the center of the ratchet and uses an extension spring to pull the pawl down and engaged to the gear. However, since the haptic mechanism must be mounted on the top of the HEDAS plates, the design is modified such that the pawl is mounted below the center of the ratchet and uses a compression spring between the pawl and the HEDAS top plate to push the pawl up and engage it to the ratchet. This configuration has the pawls normally engaged, which prevents flexion of the fingers when the servos are not actuated. In this way, the volume of the mechanism is reduced, and better suited to the application.

An extruded cylindrical interface connects the pawl to a compression spring. A ratchet and pawl mechanism is only able to rotate in one direction unless the pawl is disengaged from the ratchet. An actuator must be used to counter the force of the spring, and control the engagement/disengagement of the pawl to the ratchet, thus controlling the flexion of the finger. To achieve this, an actuator is connected to the pawl through a non-elastic string. When the string is pulled by the actuator, the pawl is also pulled away from the ratchet, thus disengaging the mechanism. When the haptic mechanism must be engaged, the actuator releases the string, so the spring is able to push the pawl and engage it to the gear. To connect the string to the pawl, a hole runs through the spring interface through which a thread can be routed. The diameter of the hole is sized to be narrow enough that a knot will not pass through the hole and instead will secure the string to the pawl.

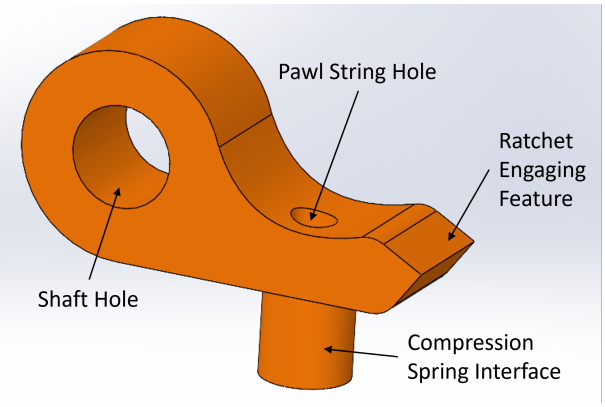

Figure 2.10: Pawl

To minimize the size of the mechanism, thin, small compression springs, similar to ones used in retractable ball point pens, are chosen. Because the pawl is small and light, the force required to push the pawl is low. Thus, it is not necessary to source springs with a high spring constant; rather, it is beneficial to utilize springs with a low spring constant because it reduces the amount of torque required by the actuator to compress the spring and disengage the pawl from the ratchet.

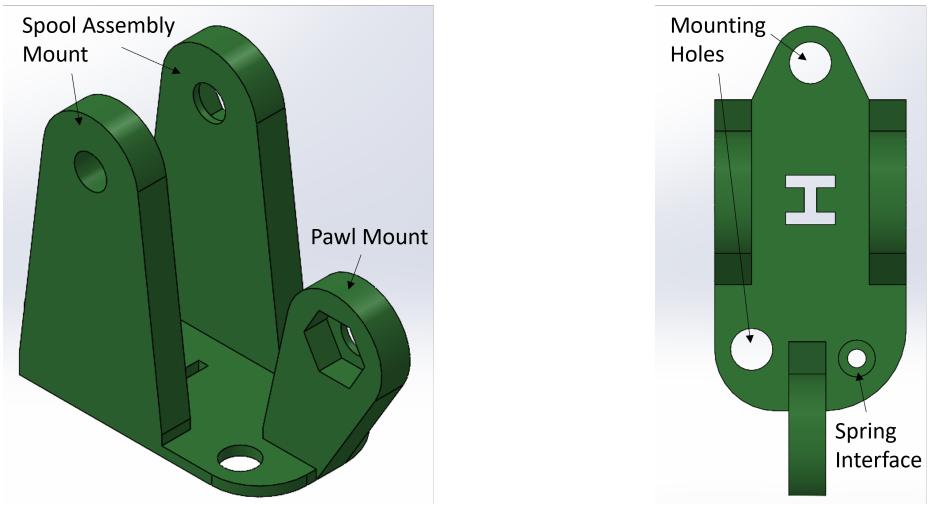

(a) Isometric View (b) Top View

Figure 2.11: Modular Base

Lastly, a base to mount the spool assembly and pawl is designed. Although the top plate could be directly modified, a separate base part that mounts to the top plate is chosen to minimize the amount of support material and time that would be needed to print the parts (design choices made with consideration for the manufacturing method are further discussed in Section 2.4). Additionally, a separate base component would allow for modularity of the haptic feedback mechanism, thus improving the ease of assembly. The base secures the other end of the compression spring using a similar cylindrical extrusion. A hole through the cylindrical feature allows the pawl string to be routed through the base and connected to an actuator. There are three pillars used for mounting on the base: two of which are used to mount the spool assembly, while one is for the pawl. One of the arms of the spool mount features a recess to press fit an M3 hex nut, which will secure the M3 bolt that will act as the shaft for the spool assembly. It is necessary to have two pillars to ensure that any axial forces from the spool spring will not be able to disassemble the spool assembly. A third and smaller pillar is used to mount and position the pawl in the correct position relative to the ratchet gear. The pawl mount also features a press fit M3 hex nut recess, which is used to

secure an M3 bolt that acts as the shaft for the pawl.

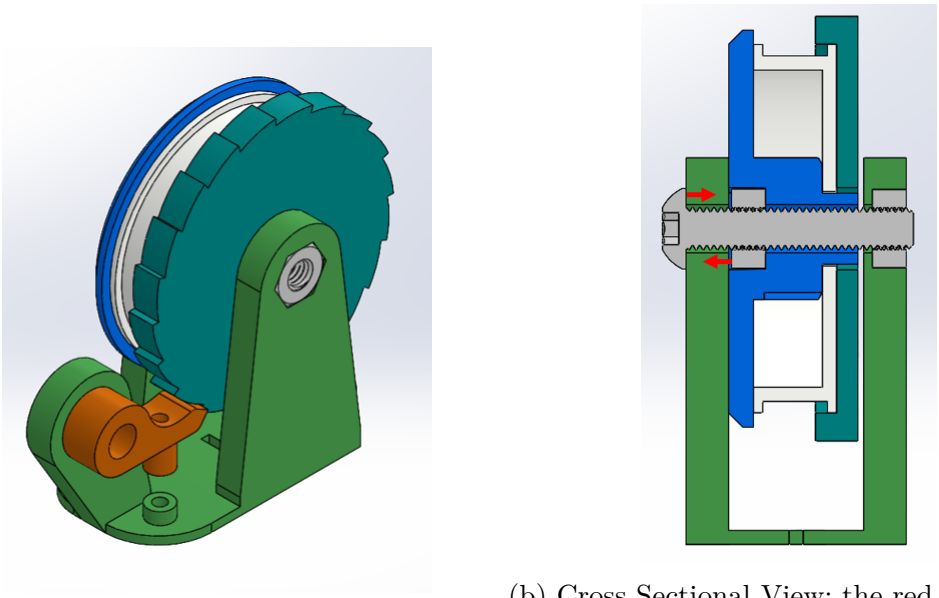

(a) Isometric View

(b) Cross Sectional View; the red arrows indicate the directions that the shaft and bolt should be secured

Figure 2.12: Modular Haptic Feedback Assembly

The assembly of a modular haptic feedback mechanism is shown in Figure 2.12a. To ensure that all of the forces from unwinding the spool are transmitted to the spring inside of the spool, and that the spool can turn smoothly, the shaft must be secured by tightening it against the spool mounting pillar closest to the bolt head, as shown in Figure 2.12b. Although it is possible to fix the shaft by tightening it against the spool pillar with the M3 hex nut, this could cause compression of the spool and gear between the shaft and the pillar. The resultant friction from the ratchet gear face rubbing against the inner wall of the spool pillar as it rotates would cause the assembly to not retract smoothly. Additionally, it is critical that the direction in which the spool is unwound is the same as the direction of rotation used to fasten and secure the shaft, so that all of the forces from unwinding are transmitted to the spring inside of the spool. If the direction of the spool unwinding is the same as the direction used to loosen the M3 screw, the force will not be transmitted to the

spring, but rather to loosen the shaft from the spool mount assembly. If this occurs, the shaft would be free to rotate with the spool and ratchet gear, so the spring would not maintain tension in the string connected to the linkages.

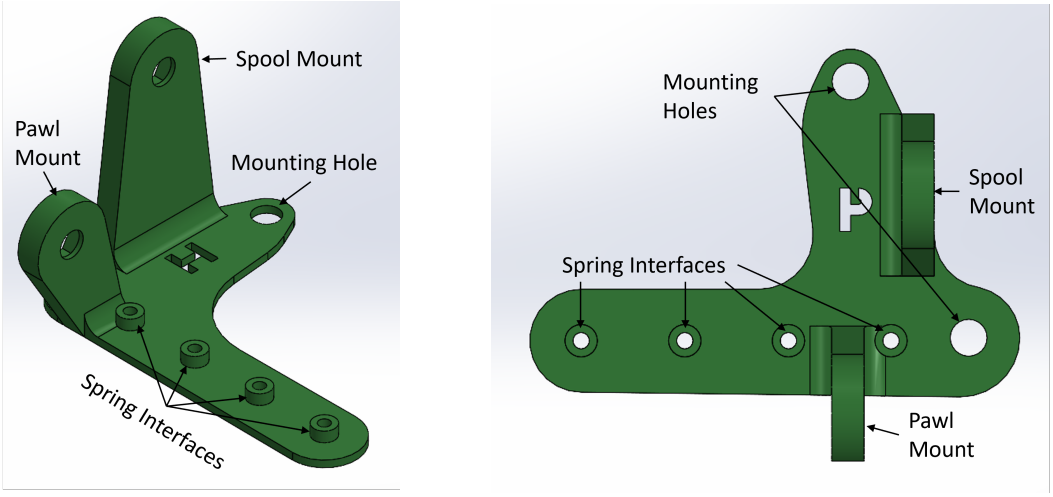

(a) Index (b) Pinkie

Figure 2.13: Multi-spool Base Components

Originally, the haptic mechanism is designed to be modular for ease of assembly. Each module, which is comprised of a spool assembly, a pawl, a compression spring, and a mounting interface, can be assembled separately from the base glove, and then mounted on the top plate. However, the modular assembly is too thick to fit eight mechanisms on the top plate, so the design is revised. Instead of relying on a pair of mounting pillars to fix the shaft of each spool assembly, all of the spool assemblies are stacked side by side on one shared M3 rod, and each shaft is tightened against the adjacent shaft. This way, the added thickness from the mounts are eliminated, allowing eight spool assemblies to fit on the top plate. Similarly, the pawls are mounted on one rod with spacers to ensure that each pawl is properly aligned with its respective ratchet. The base design is updated to accommodate for the new spool assembly arrangement, called the multi-spool assembly. The base is separated into two components: the index mount and the pinkie mount (see Figure 2.13). Together, both parts

secure the ends of the spool rod, as well as the pawl rod, and provide the interfaces for the compression springs used by each pawl.

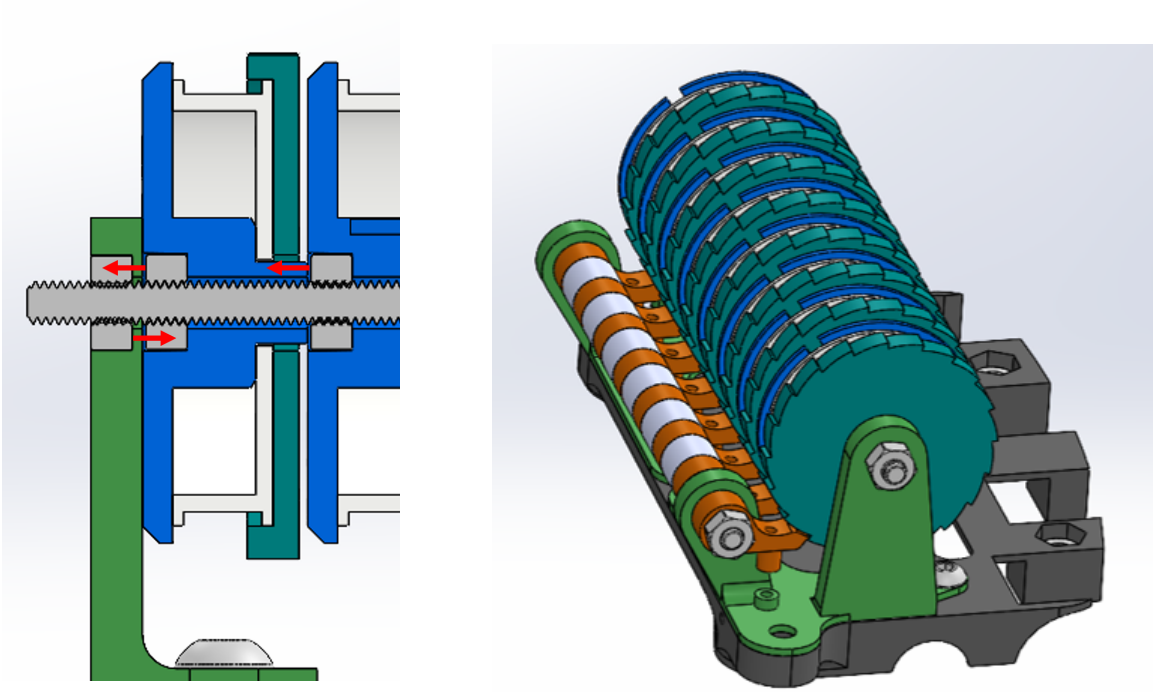

(a) Cross Section View; the red arrows indicate the directions that the nuts should be fastened

(b) Isometric View

Figure 2.14: Multi-spool Assembly

When the eight spool assemblies are mounted on a rod, the gear and shaft faces of adjacent assemblies must not contact, because the friction and compression of the gear against the shaft would impact the retraction of the spool. Therefore, the shaft length is made to be slightly longer than the thickness of the gear and spool so that a small gap will be present between each assembly and prevent binding of the gear. As shown in Figure 2.14a, the spool assembly closest to the index mounting pillar is secured by the press fit M3 nut on the outside of the pillar, and the M3 nut in the shaft. The adjacent spool assembly is tightened against the fixed shaft of the first assembly. This pattern is repeated for all spool assemblies.

To actuate the haptic mechanism, the actuator should move between two positions to engage

or disengage the pawl. Motors would require an encoder and external control loop to achieve position control, whereas servos have integrated position, velocity, and acceleration control. Therefore, a position control servo should be used. Since the locking mechanism does not rely on the power of the actuator, and the chosen spring has a low spring constant, the torque requirement of the actuator is low. Rather, the prioritized parameters of the servo are the price, weight, and size. Considered servomotors and their parameters of interest are listed in Table 2.1.

Table 2.1: Servo Motors

Servo	Cost/Unit [USD]	Weight $[g]$	Size $[mm]$	Stall Torque $[Nm]$
SG90 180° [2]	1.42	9	32.8 x 8.6 x 33.8	0.1
MG90S 180° [1]	1.75	9	32.8 x 8.6 x 33.8	0.2
GH-S37D [13]	5.00	3.7	20 x 8.75 x 22	0.07
FH-1502 Digital [7]	7.00	1.5	20.5 x 15 x 6	0.02
DM-S0020 [12]	5.00	2	16.2 x 8.2 x 15	0.02

The DM-S0020, FH-1502, and GH-S37D are top three lightest and smallest servos, but they are the most expensive and offer the lowest torques. The SG90 and MG90S are identical in size and weight, but the SG90 is slightly cheaper than the MG90S in exchange for lower torque. The DM-S0020, FH-1502, and GH-S37D are considered too expensive despite their attractive weight and size, as eight actuators are required for the design. The MG90S is opted for over the SG90 because the difference in cost is small enough that the extra power is justifiable.

2.3 Base Glove Modifications

The base glove design is modified to improve ergonomics, the assembly process, and accommodate for the haptic mechanism. For ease of assembly, the slots for the M3 nuts in the

plates and linkages are modified to be press-fit. Especially during the assembly of the plates, some of the M3 nuts cannot be accessed as they are inserted in the middle plate, which is compressed between the top and bottom plates. By providing press-fit slots, the nuts are secured in the desired position without the use of hands. Additionally, the connections to the potentiometers are modified. Originally, the design features three channels for individual wires to be placed, and the ends of the wires are to be either soldered or crimped onto the potentiometer terminals. If any of the hardware malfunctions, it is difficult to troubleshoot and replace components. Instead, off the shelf (OTS) 3-pin JST-XH connectors are used so that it is easier to assemble, troubleshoot, and replace components.

(a) Updated (b) Original

Figure 2.15: Potentiometer Holder Design

The fabric glove is removed from the design, and finger rings are used to mount the hardware to the hand instead. Fabric transmits force through tension, and due to the geometry of the glove, it is not possible to control the direction that force is transmitted through the glove. For example, in the original HEDAS glove design, the forces applied to the proximal phalanges can also be felt in the intermediate phalanges as the fabric around the proximal phalanges is pulled. By removing the fabric and opting for a ring design, the forces are transmitted only to the areas of interest. Additionally, this improves the ergonomics of the glove as users do not feel constricted by a layer of fabric that covers the entire hand. Instead, the areas of contact are minimized to only the necessary mounting points.

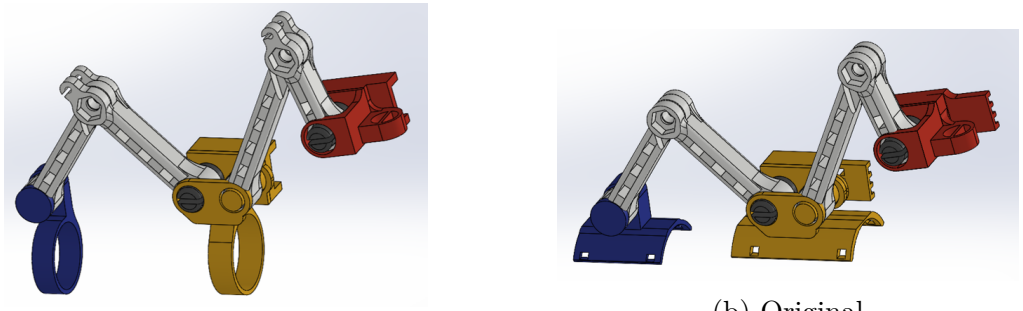

(a) Updated

(b) Original

Figure 2.16: Finger Assembly Design

To provide mounting interfaces for the haptic mechanism, the linkages connected to the potentiometers for the PIP and MCPx joints are modified to have small hooks at the ends. Hooks are opted for instead of through holes so that the strings can easily be untied from the linkages if required. With the addition of the hooks, the linkages for the finger assembly for the pinkie begins to have collision problems because the pinkie is the shortest finger. To remedy this, the one of the linkages for the pinkie is shortened to prevent collision. The top plate is modified to have guide holes for the pawl strings, mounting features for the haptic mechanism, and slots for wire routing of the potentiometer wires. Due to the large volume of wires and strings required, it is essential to incorporate design features to organize the wires and strings and prevent entanglement.

The middle plate is modified so a spool guide could be attached. The spool guide is critical for ensuring that the strings do not snag and that the force of the haptic mechanism can be transmitted through the strings in the desired direction.

Since the DOFs at the wrist are not being implemented, it is not necessary to keep the potentiometers or their respective mounting interfaces on the top plate. These features are removed so that the space could be completely dedicated to the haptic feedback mechanism.

A part is designed to mount the servos. Ideally, the servos should be mounted on the arm to

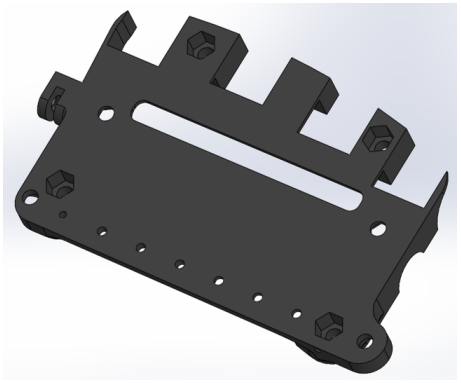

(a) Updated (Top View)

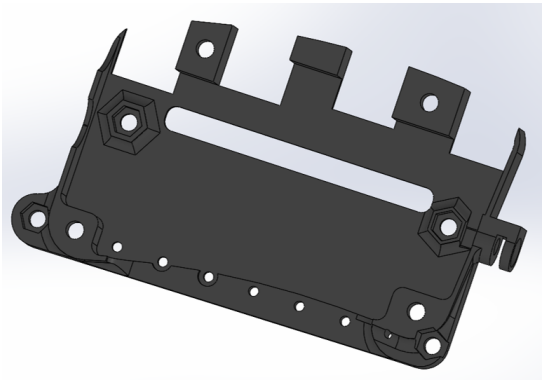

(b) Updated (Bottom View)

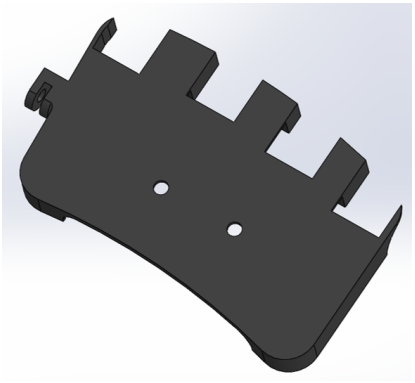

(c) Original (Top View)

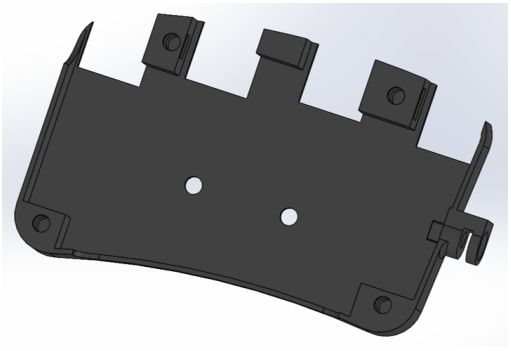

(d) Original (Bottom View)

Figure 2.17: Top Plate Design

reduce the weight of the glove at the hand, but because the actuation of the pawls requires on constant tension in the pawl string, the design of such a mounting system becomes non-trivial. A direction connection from the pawl to the servos cannot be used as the amount of tension in the string will vary depending on the rotation of the wrist and position of the hand relative to the forearm. Some means of addressing this problem are utilizing a Bowden cable, or introducing another spring-loaded spool system similar to the ratchet used to maintain tension in the strings connecting to the fingers. Unfortunately, both solutions would require more hardware, thus introducing more weight and complexity to the system. Thus, a simpler design in which the servos are mounted to the top plate is adopted, as this will ensure that the servos will maintain a constant relative position to the pawls, thus ensuring constant

tension in the pawl string.

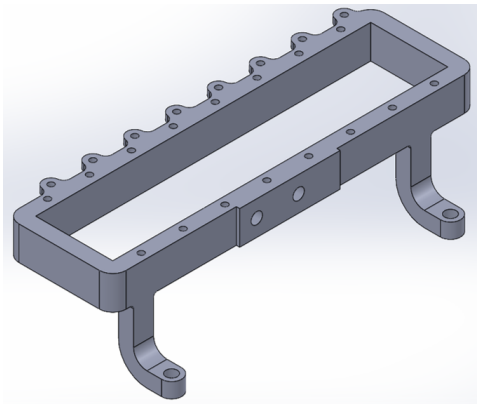

(a) Servo Mount

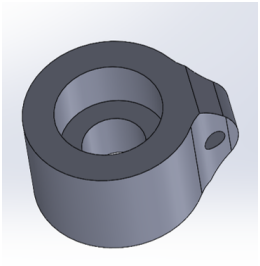

(b) Servo Attachment

Figure 2.18: Servo Interfacing Components

When mounting the servos to the top plate, it is preferable to keep the servos as close to the back of the hand as possible to minimize the torques resulting from the weight of the servos, but at the same time, the servos must be elevated so that they do not collide with the haptic mechanism, or the hand due to movement of the wrist. The screws that are provided with the servos are used to secure the servos to the mount. Eight guide holes are also located on the back of the servo mount to manage the routing of the pawl threads to their respective servos and prevent snagging or entanglement. Due to the servo mount design, an attachment for the servo needs to be designed. Given the arrangement of the servos, the original servo attachments provided are too large and would conflict with the adjacent servo. The new servo attachment is minimal ensuring no collision between adjacent servos, and features a small hole so that the pawl string can be tied to the servo.

To provide the 6 DOFs at the wrist, a mount for a VR system is designed. The mount design is dependent on the VR system used; for this thesis, the HTC VIVE system is used, so a mount that is compatible with VIVE hardware is designed. The HTC VIVE provides tracking of either hand-held controllers, or more compact trackers. Since the user is expected

Figure 2.19: VIVE Tracker [52]

to interact with the virtual environment using their hands, they would not be interacting with the buttons on the controller. Therefore, the VIVE tracker is used as the tracking device for the global position of the hand, as it is lighter and more compact. The VIVE tracker mount features a locating pin and a through hole for the mounting screw. The locating pin ensures that the VIVE tracker is mounted in a consistent orientation. The locating pin is designed as a separate part, which should be press fit into the mount, to minimize the printing time and amount of support material that would be required otherwise. To minimize the resultant torque of the weight of the tracker, the tracker is placed above the spools. The VIVE tracker is designed to be mounted to the side of the servo mount.

Lastly, the original box for the housing of the microcontroller and multiplexer is modified. Slots are introduced which could be used to secure the box to the forearm using straps, and parallel slots are introduced so that the microcontroller, multiplexer, and a breadboard PCB can be secured parallel to each other. The face of the breadboard PCB, which acts as an interface to connect the servos to the microcontroller, is exposed so that the servos can be easily connected or disconnected (the electrical design is further discussed in Chapter 3). Additionally, the orientation of the breadboard minimizes the bending and strain on the

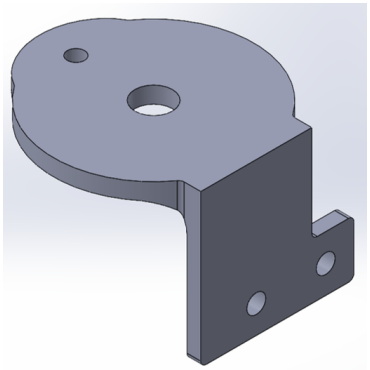

(a) Base

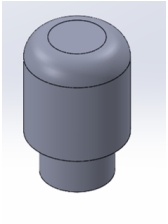

(b) Pin

Figure 2.20: VIVE Tracker Mount

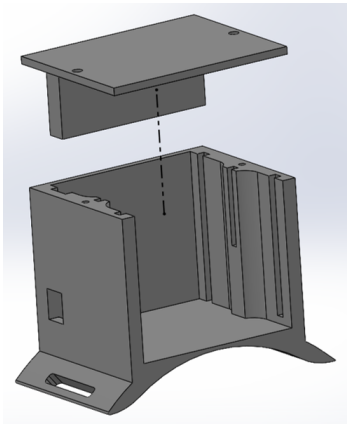

(a) Updated (Exploded View)

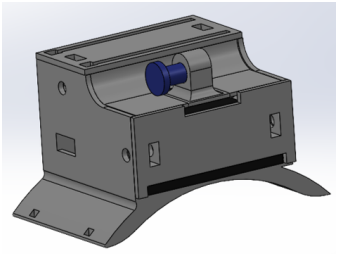

(b) Original

Figure 2.21: Electronics Box Design

wires.

2.4 3D Printing

The same manufacturing technology and material used by HEDAS are used to print the haptic mechanism components as well. Although there are several types of additive manufacturing technologies, FDM printers are the most common and popular due to their lower price and simplicity. Even if consumers do not own their own personal printers at home, 3D

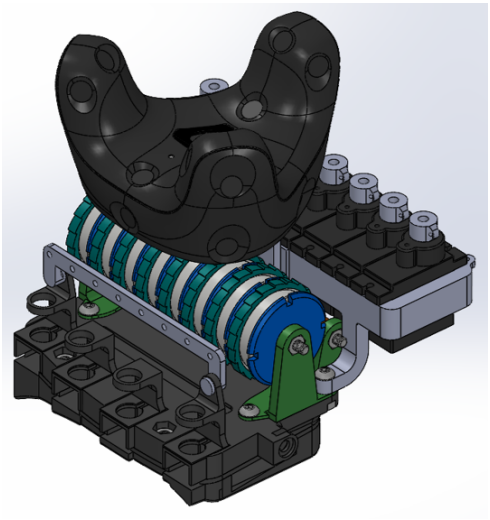

(a) Updated

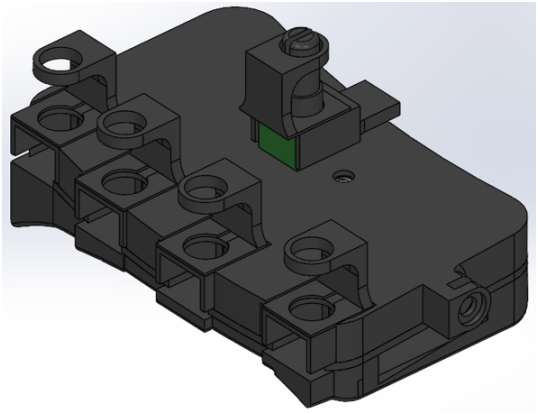

(b) Original

Figure 2.22: Plate Assembly

printing services are available at makerspaces, libraries, or online. Depending on the model and calibration of the printer, the accuracy of the printed part may vary. For this thesis, all parts are printed using the Creality Ender 3 Pro [22], which is a slightly improved model of the Ender 3 used by Aujas for the HEDAS glove. If users find that the dimensions of features, such as the press fit M3 hex nut slots, are not printed such that press fit is achieved, the CAD files should be modified and tailored to each consumer's printer such that the desired function of the feature is achieved. Similarly, the variation in human hand size makes it impossible to design finger rings that will universally fit every consumer's fingers. One of the strengths of additive manufacturing is the ease of customization of parts compared to some traditional manufacturing methods such as injection molding or casting. The finger ring diameters should be adjusted and tailored to each consumer as necessary, such that the rings fit securely around the intermediate and proximal phalanges.

For FDM printers, the some of the most common printing materials include PLA, ABS and TPU, with PLA being the most popular because it is the easiest to print. TPU is not chosen because it is an elastic material and not appropriate for the mechanism, which

requires rigidity. ABS, although stronger than PLA, is prone to warping and is much more difficult to print; since the goal of the haptic glove design is to be accessible to consumers, the manufacturing method and material should be kept as simple as possible so that parts can be printed easily by consumers without expertise in FDM printing. The material properties of PLA are sufficient to meet the requirements of the haptic mechanism, so PLA is used.

The computer aided design (CAD) files for the modified HEDAS glove and the haptic mechanism the parts are converted to STL files, which are then processed through a 3D printing software called Cura. Cura slices the desired geometries into layers and generates the instructions used by SLA 3D printers to print the desired parts. Parameters of FDM printing, such as the layer height and print orientation, are set through the settings in Cura and have noticeable impacts on the material properties and performance of the printed parts, as well as the print time and amount of printing material used.

Default layer height options in Cura are $0.28mm$, $0.2mm$, $0.16mm$, and $0.12mm$. Although lower layer heights yield more accurately printed parts, since the part is discretized into a greater number of layers, the print time becomes much longer. However, due to the detailed and miniature nature of the haptic mechanism components, such as the pawl and the ratchet gear, the accuracy of the part is crucial as it will have a direct impact on the functionality of the parts. Therefore, despite the increase in print time, a layer height of $0.16mm$ is used.

As mentioned in Section 2.2, the parts are designed with consideration for the manufacturing process. Since parts are printed in layers starting from the build plate, support material must be printed under any overhanging features to ensure that the features will not sag due to gravity when printed. Support materials use print material that is ultimately removed and discarded when the part is post-processed after printing, and adds to the printing time. Depending on the location and shape, it may be time-consuming and difficult to ensure clean removal of support material. Thus, the haptic mechanism parts, as well as the HEDAS

modifications, are designed such that the components could be printed with minimal support material (for example, designing a separate base component rather than modifying the top plate). If the generation of support material is unavoidable, then the geometry of the parts is designed such that the support material can be easily removed.

The printing orientation of the components affects the accuracy and strength of the printed parts, as well as support material generation and print time. Since the parts are printed layer by layer, the parts have anisotropic strength properties, and are more susceptible to failure when tension loads perpendicular to the layers are applied. The printing orientation also determines how the part will be sliced into layers. For example, assume that a cylinder with a diameter that is smaller than the height is to be printed. If the cylinder is printed horizontally, it will be sliced into rectangles of varying widths, while the same cylinder will have identical circular cross sections for each layer if printed vertically. The vertically printed cylinder will have better accuracy than the horizontally printed cylinder because the cylindrical surface is not discretized, but the print time for the horizontal orientation will be shorter than the vertical as it will be printed in fewer layers. Lastly, a part may have overhanging features when printed in one orientation versus another. Therefore, the printing orientation of the components are chosen in a way that carefully balances minimizing support materials and print time, while maximizing accuracy and strength. The total bill of materials (BOM) that must be 3D printed for the assembly is provided in Table 2.2. The orientations used to print all of the components are shown in Figure 2.23.

The thumb assembly, although present in the CAD, is omitted during the printing and assembly of the design as the purpose of this thesis is to discuss the design of a mechanism that provides feedback to the index, middle, ring, and pinkie fingers. The thumb assembly may be printed and included in the assembly for the full design (see Table 2.3 for the BOM of 3D printed parts for the thumb). The total print time without the thumb assembly is $45h$

and $57min$ and uses $172g$ of PLA. With the thumb, the total print time would be $53h$ and $30min$, using $193g$ of PLA. If a coarser layer height is used, the required time is expected to drop significantly, but it is unclear whether the reduction in accuracy would impact the functionality of the printed parts.

Table 2.2: 3D Printed Parts BOM

Sub-Assembly	Part Name	Qty
Finger	Wire Holder MCPx	4
	Bar Connection Small (including Pinkie Version)	4
	Bar Connection MCPx	4
	Bar Connection	4
	Bar Connection 2	4
	pin PIP	4
	Revolute Joint Holder PIP	4
	Revolute Joint Holder	4
	Wire Holder PIP	4
Servo	Servo Mount	1
	Servo Attachment	8
Plate	Bottom Plate	1
	Middle Plate	1
	Top Plate	1
	Multi-spool Thread Guides	1
	Multi-spool Thread Guides Pin	1
Haptic Feedback	Multi-spool Base Index	1
	Multi-spool Base Pinkie	1
	Pawl	8
	Pawl Standoffs (Regular Length)	6
	Pawl Standoffs (2.5mm Extra Short)	1
Spool Assembly	Ratchet Gear	8
	Shaft	8
Electronics Box	PCB Wrist Mount	1
	PCB Wrist Mount Cover	1
VIVE Tracker Mount	VIVE Tracker Mount Base	1
	VIVE Tracker Mount Pin	1

Table 2.3: Thumb 3D Printed Parts BOM

Sub-Assembly	Part Name	Qty
Thumb	Wire Holder CMC x	1
	Bar Connection Small (Original Version)	1
	Bar Connection MCPx	1
	Bar Connection (Original Version)	1
	Bar Connection 2	1
	pin PIP	1
	Revolute Joint Holder PIP	1
	Revolute Joint Holder	1
	Wire Holder PIP	1
	Wire Holder CMC z	1
	Wire Holder MCPz	1
	CMCy	1
	Test Bar CMC y	1
	Test Bar CMC	1
	Test CMC x Bar	1

Table 2.4: 3D Print Times and Material Usage

Print File	Print Time [h:min]	Print Material [g]
Finger	15:14	45
Haptic Feedback & Spools	7:59	34
Plate & Servo	16:01	54
Electronic Box & VIVE Mount	6:43	39
Thumb	7:33	21
Total (without Thumb)	45:57	172
Total (with Thumb)	53:30	193

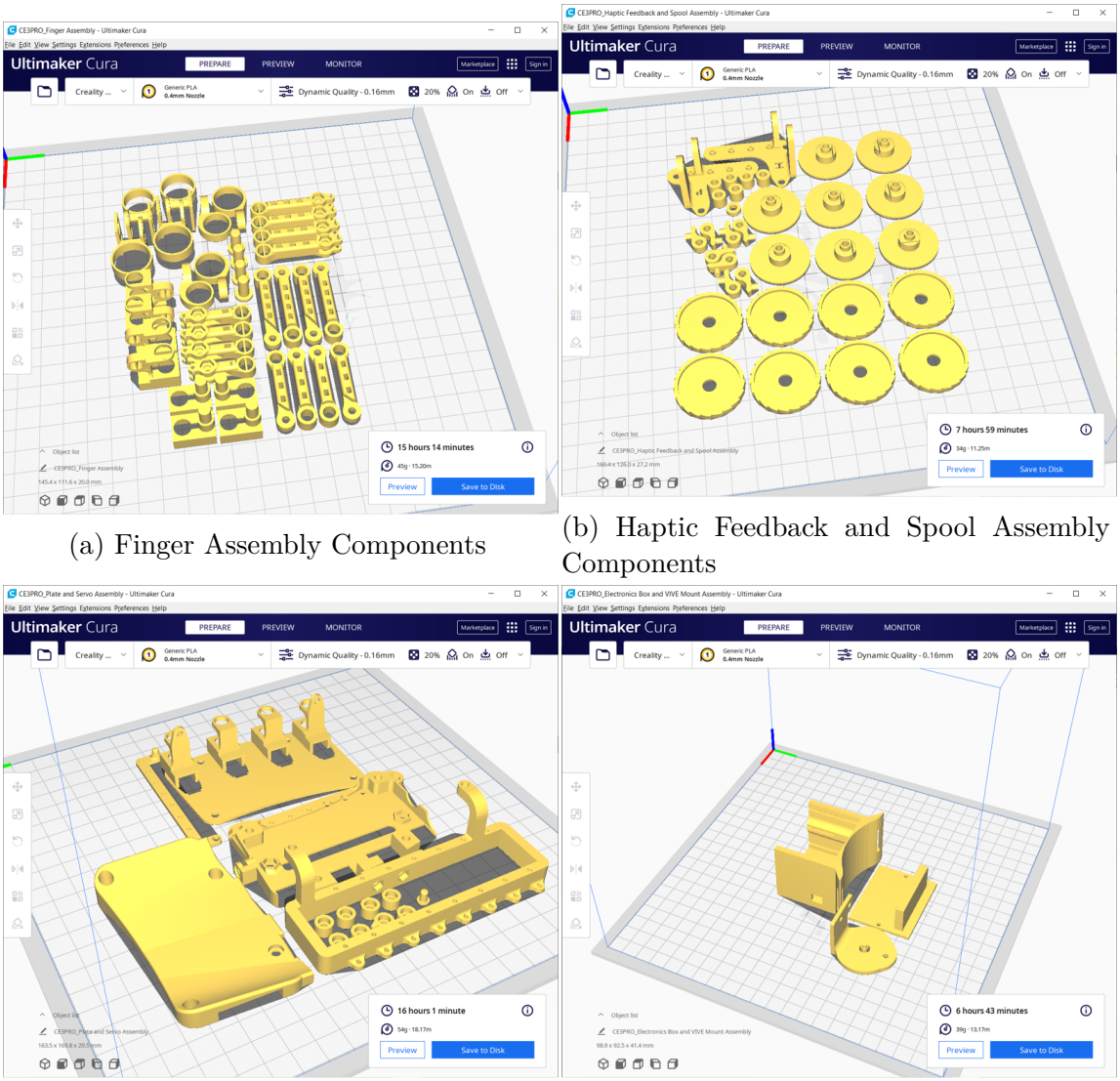

(a) Finger Assembly Components

(b) Haptic Feedback and Spool Assembly Components

(c) Plate and Servo Mount Assembly Components

(d) Electronics Box and VIVE Mount Components

Figure 2.23: 3D Printing Orientation

Chapter 3

Logic and Controller Implementation

3.1 Electrical Design

The HEDAS glove utilizes a generic reproduction of the Arduino Nano (referred hereon as the Nano), which is functionally identical to the official Arduino Nano, but much cheaper due to the lack of branding. The Nano has 14 digital general purpose input/output (GPIO) pins and eight analog pins, of which four digital and six analog pins are used for the HEDAS glove (the original design utilizes all eight analog pins, but since the wrist DOFs have been removed, two of the analog pins are no longer used). Since there are enough digital pins remaining that could be used to actuate the servos of the haptic mechanism, it is not necessary to select a larger microcontroller.

The circuit diagram for the haptic feedback mechanism is provided in Figure 3.1. The servos are connected in parallel to a portable external power supply, such as a portable power bank for phones. The servo signal pins are connected to the remaining digital pins on the Nano. Most recent power banks have built in auto-off features which prevents power output from the power bank if the current draw is below a threshold. Therefore, it is recommended that an older generation power bank without an auto-off feature is used. If an auto-off power bank must be used, the current drawn by the servos is not enough and the power bank will shut off, so the addition of a resistor in parallel with the servos is necessary to keep the current draw above the threshold. The threshold current ($I_{\text{threshold}}$) varies depending on

the power bank used, so the resistance that should be used will also vary. The resistance required to prevent the power bank from shutting off ($R_{\text{auto-off}}$) can be determined by

$$R_{\text{auto-off}} = \frac{5}{I_{\text{threshold}}}. \tag{3.1}$$

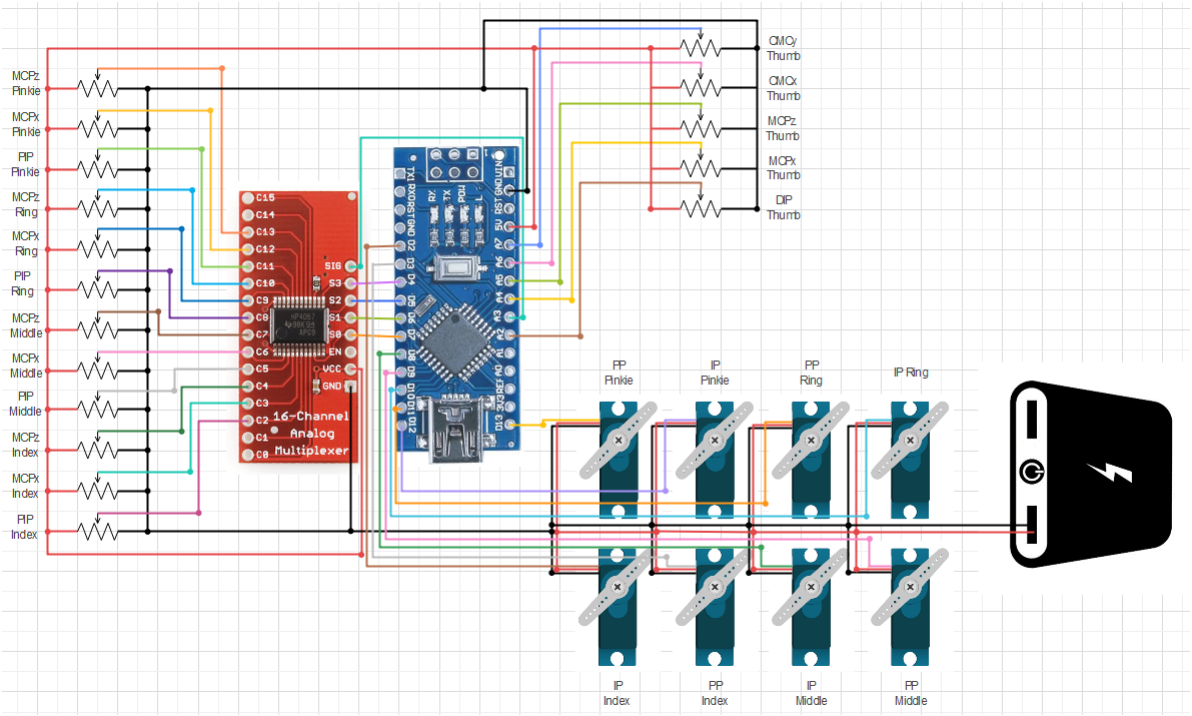

Figure 3.1: Circuit Diagram; MCPx is the DOF responsible for flexion/extension, MCPz is the DOF responsible for adduction/abduction. IP = Intermediate Phalanx, PP = Proximal Phalanx

This is a rudimentary solution that wastes power, but optimized solutions should be considered in future work.

The current draw of a servo during actuation typically ranges from 120 to 250mA [43]. Taking the worst-case scenario, if all eight servos are drawing 250mA simultaneously, the total current that must be supplied by the power bank is 2A. A power bank with an output of at least 2A should be chosen; the operation time on one charge should be at least 1h,

Table 3.1: Power Banks (all considered options are able to output $2A$ at $5V$)

Brand	Capacity $[mAh]$	Dimensions $[mm]$	Weight $[g]$	Cost/Unit [USD]
INIU [10]	10000	105 x 66 x 24	195	24.99
Anker [4]	5000	130 x 100 x 30	98	31.99
INIU [9]	10000	132 x 69 x 13	198	19.96
FOCHEW [8]	20000	150 x 75 x 15	250	14.98
Charmast [6]	10000	90.5 x 62 x 22.2	187	29.99
Anker [3]	5000	107 x 33 x 33	136	17.99
Anker[5]	5200	96 x 45 x 23	128	24.99
Miady [11]	5000	91 x 64 x 10	119	7.00

so the capacity should be at least $2000mAh$. Additionally, the power bank must be able to provide $5V$, which is the nominal voltage of the servos. Other factors that are considered in the selection of a power bank includes the price, dimension, and weight. Table 3.1 lists the power banks that are considered, and their specifications. The $5000mAh$ power bank by Miady is used for this thesis, as it is the most economical option and has one of the smallest dimensions. However, the power bank selected is just a suggestion that can be exchanged with a different option. For users who desire longer operation on one charge, power banks with higher capacities should be used; ultimately, the power bank selection should be tailored to each consumer's needs.

A small soldering breadboard is used as an interface to connect multiple wires to a single node, such as the power and ground wires of the potentiometers. Additionally, male header pins are soldered to provide an interface for the servo connectors. The schematic of the breadboard is shown in Figure 3.2.

The design relies on soldering to ensure that the connections are secure and to minimize the size of the electrical components. Most consumers do not own a personal soldering iron, but the recent surge of popularity in DIY and accessibility of 3D printers has prompted some public libraries to create makerspaces, which library patrons can use, or provide soldering

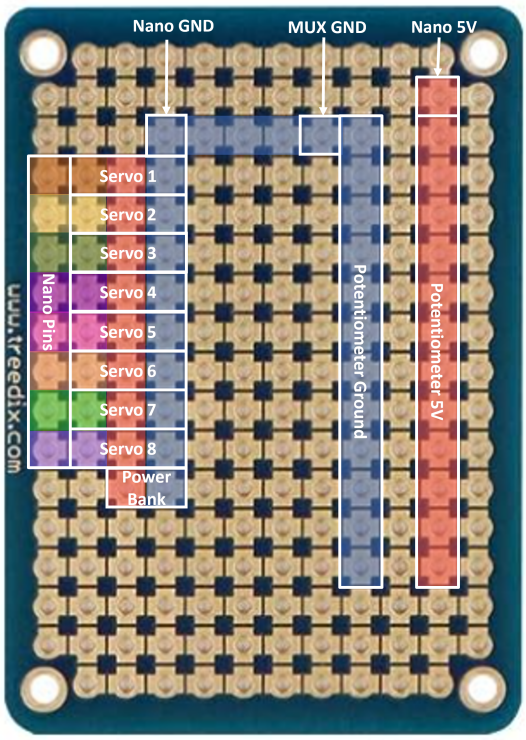

Figure 3.2: Breadboard Schematic; the blocks of colour indicates electrically connected through-holes. Red = $5V$, blue = ground, any other colour = servo signal

irons that can be borrowed. Independent maker spaces have also emerged, where consumers can buy memberships to gain access to the equipment, which often include soldering irons and 3D printers. Thus, it is possible for consumers without this equipment to gain access to them. Alternatively, if it is not possible to solder connections, substitutions can be made, such as using terminal blocks, connectors, or an insertion breadboard instead of a soldering breadboard.

3.2 Calibration

The mounting locations of the finger linkages on the user's finger will differ with each use. This discrepancy will vary the mapping between the potentiometer resistance to the actual

joint angle of the hand; to address this, the original design includes an Arduino sketch and Python script which work together to calibrate the glove. The Arduino sketch is responsible for interfacing with the 16-channel analog multiplexer to provide the values recorded by the analog to digital converter (ADC) to the Python script. During the calibration stage, the user is prompted to perform five specific poses with their hand. At each pose, the values of the potentiometers are recorded and used to determine the mapping between the value and the joint angle. Since the fourth and fifth calibration poses are required to calibrate the wrist, these steps are omitted for the calibration of the haptic glove. There is a second degree relationship between the resistance of the potentiometers responsible for measuring the angles of the PIP and MCPx joints, because the joints of the glove are offset from the actual joints that are being measured, while the MCPz joints have a linear relationship with their respective potentiometers. The HEDAS python script determines the conversions from ADC values to joint angles through second order polynomial curve fitting of the PIP and MCPx joints, and linear mapping of the MCPz joints. Once the calibration steps are completed, the mapping settings are saved. In future sessions, users may choose between using a previous calibration or completing a new calibration. After calibration, the script converts new incoming ADC values to their respective joint angles and begins to send the data, which is stored in an array, to an executable through a socket. The executable is used in Aujas' work to validate the performance of the HEDAS system.

A calibration Arduino script is used to determine the positions that the servos should turn to engage or disengage the pawls from the ratchets. The method in which the pawl strings are fixed to their respective servos can vary, which will impact how much the servos must pull to achieve enough tension to actuate the pawl. The calibration script simply has the servos move between two positions so that the user may experimentally determine what angular positions will work for their assembly.

3.3 Haptic Feedback Logic

The original HEDAS python and Arduino scripts are modified to incorporate haptic feedback. After the Nano reads the potentiometer values and sends the data in an array to the python script, the python script forwards the data to a computer generated environment, instead of the HEDAS executable. The environment will update the pose of the virtual hand to mirror the user's hand using the joint angle data, and then compute for any collisions between the new hand pose and objects in the environment. The environment should return the new collision data to the python script, which will relay the data back to the Nano. The Nano will read the collision data and actuate the servos accordingly.

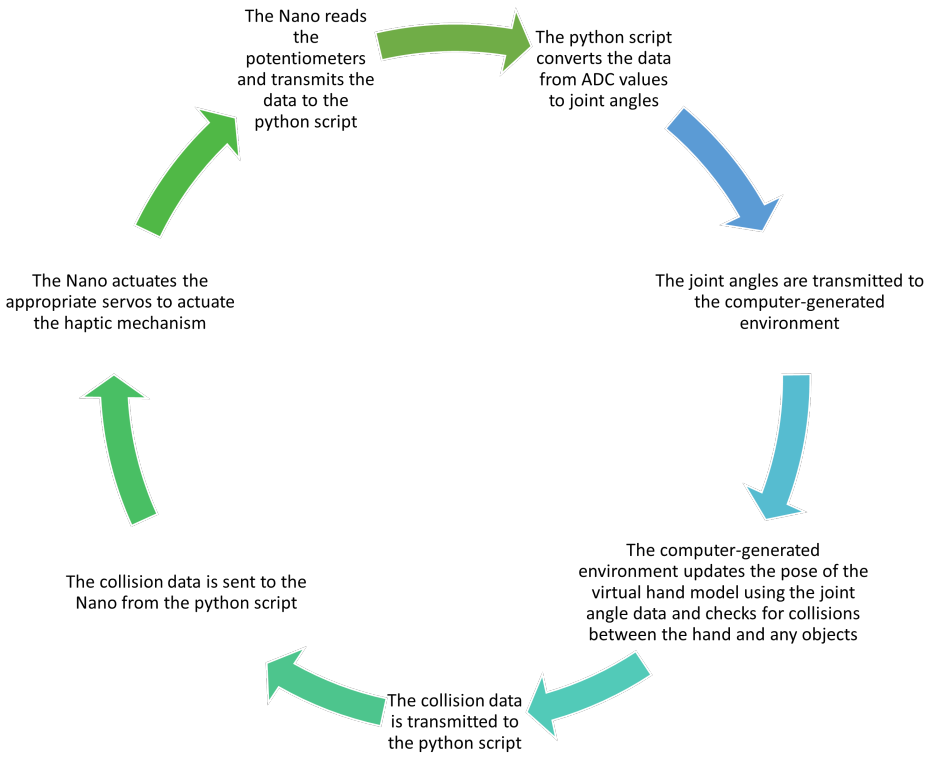

Figure 3.3: Flowchart of the Haptic Feedback Mechanism

Ideally, the Nano should transmit the potentiometer readings while reading the collision

array and actuating the necessary servos simultaneously, but because the Nano features a single core processor, it is not possible to run multiple tasks in parallel. Often, interrupts are used in microcontrollers to mitigate this issue but, for this application, interrupts would introduce unwanted errors. Transmitting and receiving data over serial communication is a relatively time-consuming task compared to other functions, so it is possible that if an interrupt occurs in the middle of a set of potentiometer readings, a discrepancy could occur where the first half of the readings that occur before the interrupt represent a completely different hand pose than the readings that occur after the interrupt. To prevent this issue, the code is intentionally designed to be sequential. The pose of a hand at a given time is fully read and transmitted by the Nano, which then waits to receive a collision array. Once the response is received and the corresponding actuation is completed, the Nano will repeat this loop. Because the clock speed of the Nano is $16MHz$ [15], it is expected that a sequential flow will not impact the latency of the system enough to be detected by the user. In literature, human reaction time standards for computer-human interfaces are typically $200ms$ per loop [41]; any latency below this threshold value is unnoticeable and seems instantaneous to the user. Therefore, the system is acceptable as long as the latency is less than $200ms$.

Chapter 4

Cost

The BOM for the glove is provided in Table 4.1. The cost of the 3D printer and any tools, such as a soldering iron, hex keys, and wire cutters, are not included. If the user owns an Ender 3 or Ender 3 Pro, the glove can be assembled with all of the tools provided with the FDM printer. Due to time constraints, most of the parts for the glove are sourced from Amazon. However, the parts are sold for much cheaper by other retailers such as AliExpress, which could be used if lead times for receiving parts are not a concern.

The total cost of the gloves shown in Table 4.1 is $224.89. However, most of the components are sold in bundles that contain quantities that are double what is needed to build one glove. When the cost is computed based on the per-unit cost using the exact quantities required, it can be seen that the cost of a single glove is significantly cheaper. Note that the "cost per unit" of the PLA is the cost per gram rate, and the "quantity" used is the total mass of PLA as discussed in Section 2.4. For quantities that cannot be quantified, such as the amount of WD40 and solder used, the required quantity is assumed to be the full amount, but it is likely that less than a quarter of the amount of the WD40 and solder would be used.

Table 4.3 shows the cost of the glove if all of the materials are purchased from a cheaper retailer such as AliExpress, with the exception of the WD40 lubricant, which is not available from that retailer. The prices listed are the full, non-discounted prices, but many of these items are typically sold at discounted prices.

Table 4.1: Bill of Materials with Links

Item	Qty	Cost [USD]	Link
20 pcs 0.3 x 4 x 10mm Stainless Steel Compression Springs	1	9.49	Amazon
50 pcs Retractable Badge Reels	1	16.95	Amazon
12 pcs MG90s Micro Servo 180°	1	20.99	Amazon
400 pcs M3 Screws and Nuts Assortment Kit	1	11.97	Amazon
2 pcs Power bank	1	13.99	Amazon
20 pcs JST-XH 2.54 3 Pin Connector with 200mm Wire	1	8.59	Amazon
WD40 Multi-purpose Lubricant 3oz	1	3.98	Walmart
5pc M3 x 0.5 x 90mm Threaded Rod	1	7.19	Amazon
20 pcs Cable Straps	1	8.99	Amazon
25 pcs 1/4-20 x 3/4” Bolt	1	7.99	Amazon
2 pcs USB Cable	1	8.80	Amazon
Phone Arm Band	1	9.99	Amazon
PLA 3D Printer Filament (1kg)	1	24.99	Amazon
3 pcs Nano Board	1	19.99	Amazon
16-Channel Analog Multiplexer	1	5.69	Amazon
9 pcs Mini Solderable Prototype Shield Board	1	10.99	Amazon
10 pcs 10k Ohm Rotary Potentiometer	2	25.32	Amazon
Solder	1	8.99	Amazon
Total cost		224.89	

Ideally, if the components for the glove are purchased on Aliexpress, the cost of the glove is $73.07, which is significantly lower than the cost of a commercial glove, and falls in the lower end of the $68.79 to $137.57 USD price range deemed reasonable by surveyors in Aujas [16]'s market research.

Table 4.2: Bill of Materials per Unit

Item	Cost/Unit [USD]	Qty	Total Cost [USD]
0.3 x 4 x 10mm Stainless Steel Compression Springs	0.47	8	3.80
Retractable Badge Reels	0.34	16	5.42
MG90s Micro Servo 180°	1.75	8	13.99
M3 Fasteners (18 screws, 22 nuts)	0.03	40	1.20
Power bank	7.00	1	7.00
JST-XH 2.54 3 Pin Connector with 200mm Wire	0.43	12	5.15
WD40 Multi-purpose Lubricant 3oz	3.98	1	3.98
M3 x 0.5 x 90mm Threaded Rod	1.44	2	2.88
Cable Straps	0.45	2	0.90
1/4-20 x 3/4" Screw	0.32	1	0.32
USB Cable	4.40	1	4.40
Phone Arm Band	9.99	1	9.99
PLA 3D Printer Filament	0.02	172	4.30
Nano Board	6.66	1	6.66
16-Channel Analog Multiplexer	5.69	1	5.69
Mini Solderable Prototype Shield Board	1.22	1	1.22
10k Ohm Rotary Potentiometer	1.27	17	21.52
Solder	8.99	1	8.99
Total cost			107.41

Table 4.3: Bill of Materials with AliExpress Links

Item	Qty	Cost [USD]	Link
20 pcs 0.3 x 4 x 10mm Stainless Steel Compression Springs	1	1.28	AliExpress
Retractable Badge Reel	16	2.72	AliExpress
MG90s Micro Servo 180°	12	11.76	AliExpress
50 pcs M3 x 0.5 x 8mm Button Head Hex Screw	1	0.39	AliExpress
50 pcs M3 x 0.5 x 10mm Button Head Hex Screw	1	0.41	AliExpress
50 pcs M3 x 0.5 x 6mm Button Head Hex Screw	1	0.37	AliExpress
20 pcs M3 Hex Nut	2	0.70	AliExpress
8000mAh (5V 2.1A Output) Power Bank	1	7.08	AliExpress
10 pcs JST-XH 2.54 3 Pin Connector with 200mm Wire	2	2.58	AliExpress
WD40 Multi-purpose Lubricant 3oz	1	3.98	Walmart
2 pcs M3 x 0.5 x 90mm Threaded Rod	1	1.09	AliExpress
5 pcs Cable Straps	1	1.50	AliExpress
3 pcs 1/4-20 x 3/4” Bolt	1	1.09	AliExpress
USB Cable (0.5m)	1	1.59	AliExpress
Phone Arm Band	1	7.48	AliExpress
PLA 3D Printer Filament (1kg)	1	15.65	AliExpress
Nano (Un-soldered Pins, No Cable)	1	2.65	AliExpress
Micro USB Cable for Nano	1	0.25	AliExpress
16-Channel Analog Multiplexer	1	0.60	AliExpress
Solderable PCB Breadboard (Mini Sized)	1	0.78	AliExpress
10 pcs 10k Ohm Rotary Potentiometer	2	3.20	AliExpress
Solder	1	5.92	AliExpress
Total cost		73.07	

Chapter 5

Assembly

The method for assembly of the glove and simulation (discussed in Chapter 6) is outlined in this section.

Tools:

- M3 Hex Key (size 2 for M3 button heads) or hex screwdriver (a key is strongly recommended over a screwdriver, though it is possible with the latter)
- 1/4-20 Hex Key
- Thin double-sided wrench (for fastening the potentiometer nuts)
- Wire cutters or scissors (for cutting spool strings)

Optional but highly recommended:

- Tape
- Twist ties
- Marker

Optional: Fine grade sand paper

Preface: It is highly recommended that all electronic components (potentiometers, servos, MUX, and Nano) should be thoroughly tested and validated individually before assembly,

as it will streamline the assembly process and minimize the need to disassemble/reassemble components to fix wiring or replace broken/faulty electrical components. Additionally, the power bank and VIVE tracker should be fully charged and operational.

1. Clean the 3D printed parts of their support materials thoroughly. Sand the parts with a fine-grain sandpaper if necessary. Press fit M3 hex nuts into all of the components that require it.

2. Optional, but highly recommended: lubricate the potentiometers with WD40. Turn the knobs of the potentiometers to work the lubricant into the potentiometers and reduce the stiffness of the knobs. If lubricated correctly, the potentiometers should be much easier to turn. Because WD40 is flammable, it is extremely important that any excess WD40 is cleaned thoroughly from the rest of the potentiometer surfaces, particularly at the potentiometer pins which will be connected to circuitry later on.

3. Assemble the linkages for the 4 fingers. The fingers are almost all identical, but they have different sized finger rings, and one of the linkages for the pinkie is slightly shorter than the rest of the fingers. For further clarification on the assembly of the finger linkages, the thesis by Aujas [16] should be referenced.

4. Assemble the 4 finger linkage chains to the middle plate. For further explanation, the thesis by Aujas [16] should be referenced.

5. Wire the JST-XH connectors to all of the potentiometers, ensuring that all of the wires are being routed properly (e.g. the wires should not be crossing over other fingers). Take the ends of the PIP and MCPx wires and feed them through the appropriate top plate holes. Ensure that none of the wires are being pinched. At this point, it is highly recommended to organize the wires by securing them from a single finger with twist

ties, and labelling all of the wires with the joints they are connected to. The labels should be placed near the exposed wire end, so that they will be accessible.

6. Align the top plate to the middle plate, and hold it in place. Flip the assembly over, and place the bottom plate over the middle plate by aligning the mounting holes. Fasten the plates together using four M3x0.5x8mm screws.

7. Flip the assembly over again, so that the top plate is facing up. Press fit the spool guide to the middle plate mounting hole, and secure the other end using the press fit pin.

8. Set the hand assembly aside and start assembling 8 spool assemblies. Break apart 16 badge reel spools, and extract eight white spool with the wound thread and coil spring attached. For the remaining eight, extract only the threads, with the knot on one end intact.

9. Press fit the ratchet gear to the flat side of the spool. Gently grab the end of the coil spring, while holding the rest of the spring in place inside of the spool. Snip off the excess spring after the first bend. If necessary, straighten out the spring enough to slide it into the slot in the shaft. Push the shaft as far as it can go towards the end of the coil. The bend at the end of the coil should stop the shaft from sliding any further. Ensure that the end of the coil spring is curved around the shaft and does not stick out in a way that would cause friction with the rest of the coil.

10. Once all eight spool assemblies are built, ensure that each one can spin smoothly. Then, using a small piece of tape, secure the wound string to the spool assembly, so that it will not unwind.

11. Screw a M3x0.5x90mm threaded rod into the index multi-spool base (MSB), just until the rod is fully engaged with the M3 nut press fit into the index MSB. For the pawl

arm, screw a M3x0.5x90mm threaded rod into the index MSB just until the rod is fully engaged with the press fit M3 hex nut. Add the spool assemblies one at a time, spinning them down the length of the rod until they can be secured by tightening the shaft. Then, add eight pawls and pawl spacers as appropriate. The shaft of each spool assembly should be closer to the index MSB, while the ratchet gear should be closer to the pinkie MSB. The sequence of the components is shown in Figure 5.1. Then, add four springs to engage the first four pawls from the left to its respective ratchet gear. Thread four of the eight strings from step 8 through the pawls and the aligning index MSB holes, pulling all the way through until the knot at the end of each string catches at the top of the pawl. Ensure that each pawl thread is routed appropriately and not tangled with the other strings.

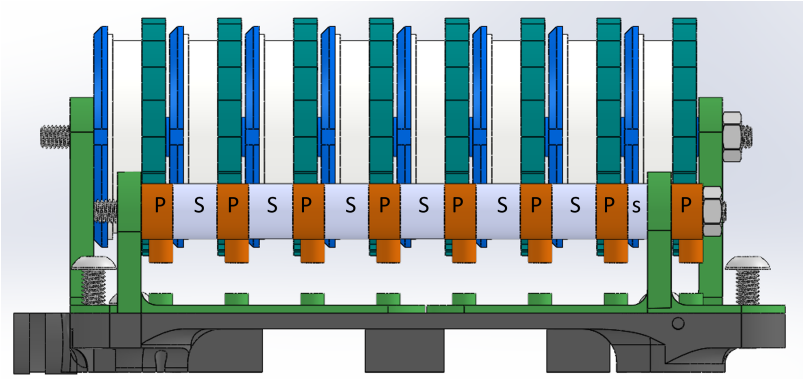

Figure 5.1: Pawl Assembly; P = pawl, S = regular length spacer, s = short spacer

12. Once all eight spools and pawls have been mounted, slide the remaining length of the rods through the respective holes of the pinkie MSB. Finally, secure the entire assembly with two M3 hex nuts on the other side of the pinkie MSB. Ensure that the nuts are not over-tightened, as this will compress the spools and pawls, which will inhibit smooth rotation. Then, add the remaining four springs to engage the last four pawls from the left to its respective ratchet gear. Thread the last four strings from step 8 through the pawls and the aligning pinkie MSB holes, pulling all the way through until the knot

at the end of each string catches at the top of the pawl. Ensure that each pawl thread is routed appropriately and not tangled the other strings.

13. Remove the pieces of tape from each spool, and unwind an appropriate length of string. Thread the strings through the respective holes of the thread guides. Then, thread the pawl strings through the aligning top plate holes, ensuring that each pawl thread comes out through the opening between the top and middle plate, and is routed appropriately (not tangled with the wires and other strings).

14. Without fastening, place the MSB/rod/multi-spool/pawl assembly on top of the top plate, ensuring that the threads do not slip out of the thread guides. Set the assembly aside, and mount eight servos to the servo mount using the flange screws provided with the servos. Ensure that the wires to the servo are extending to the back, not to the front of the hand.

15. Press fit the VIVE tracker locating pin to the VIVE tracker mount. Then, use the locating pin and the mounting hole to mount the VIVE tracker to the top of the mount using a 1/4-20x3/4" hex screw. Attach the VIVE tracker mount to the servo mount using two M3x0.5x8mm screws.

16. Mount the MSBs to the top plate using two M3x0.5x6mm screws for the front two holes. For the two rear holes, align the mounting holes of the servo mount with the servos over the two holes of the MSB. Use two M3x0.5x10mm screws to secure the servo mount and the MSBs to the top plate.

17. To attach the servo attachments, first use the servo positioning Arduino sketch to turn each servo to the 180° position. Then, attach the servo attachments to each servo, as shown in Figure 5.2, which will ensure that the direction of the attachment is aligned with the range of the servo's rotation. Secure the attachment using the screw

provided with the servo. Then, route the pawl strings to the servos, threading the strings through the respective guide holes on the back of the servo mount, and attach the end of the string to the servo attachments using a secure knot.

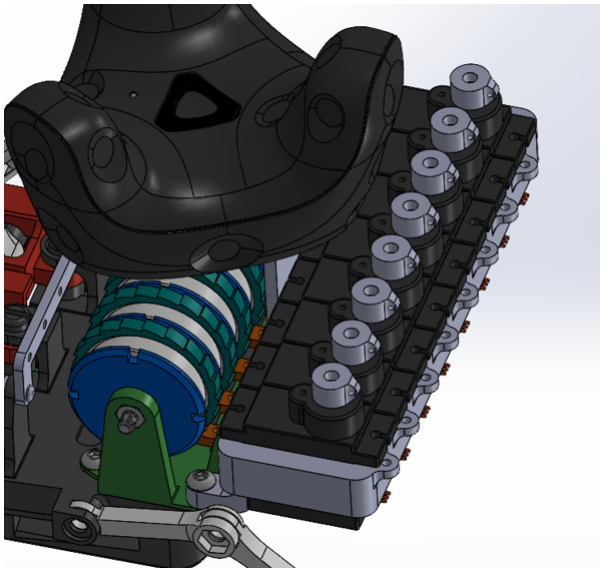

Figure 5.2: Servo Attachment Positioning

18. For the spool strings, pull and hold the respective pawl string to disengage the pawl from the spool. Then, pull the spool string slightly to engage tension in the string, and secure the spool string to the respective linkage hook using a strong knot. The strings should be routed such that they are aligned with the finger linkages as much as possible, and tied such that the tension on the two hooks of the respective linkage is distributed as evenly as possible. The routing of the pawl and spool strings are shown in Figure 5.3.

19. Feed a cable strap through the gap between the middle and bottom plate. Tighten the strap until it will hold the plate to the back of the user's hand snugly when the strap is worn across the middle of the palm. The bottom of the strap should contact the purlicue (space between the thumb and index finger).

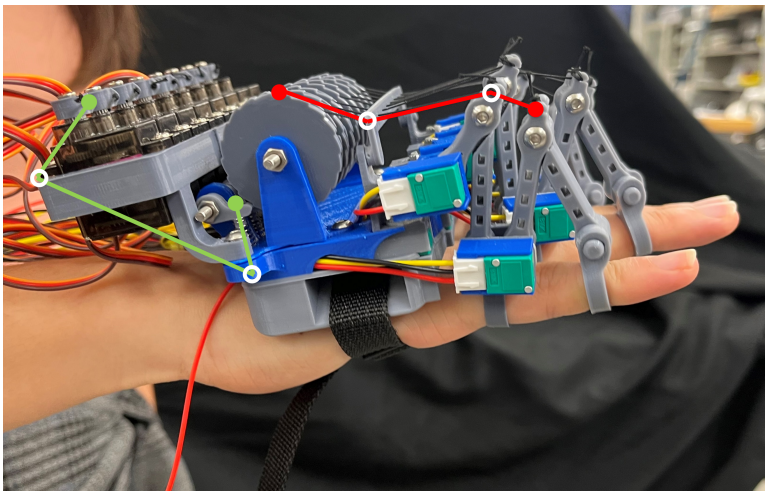

Figure 5.3: Pawl and Spool String Routes; red lines = spool strings from the PIP linkage, green lines = pawl strings. Solid filled circles = fixed mounting points, white hollow circles = routing pivot points. The spool string routing from the MCP linkage follows the same path as the routing of the string from the PIP linkage, but is mounted and terminated at the MCP linkage instead of using it as a pivot point.

The mechanical assembly of the glove is complete. Next is the electrical assembly:

1. Solder the potentiometer wires to the breadboard and MUX to reflect the schematic provided in Figures 3.1 and 3.2.

2. Break the male header pins that are provided with the Nano into sets of three pins, and solder the pins to the bread board according to the schematic shown in Figure 3.2. Connect the servo connectors to the appropriate header pins. Solder the wires of the USB cable to the breadboard to reflect the schematic, and connect the USB end of the cable to the external power bank that is mounted on the arm using the phone arm band.

3. Lastly, solder the connections from the Nano to the MUX and the breadboard, for the servo signals. Any extra lengths of wire can be trimmed from the JST-XH connectors and used.

4. Once the electrical components have been assembled, the MUX, breadboard, and Nano can be placed into the 3D printed enclosure for the electronics. The electronics box should be mounted on the forearm, close to the wrist and the rest of the glove, using the cable straps.

5. Optional: At this point, the servos should be tested to ensure that they can engage the pawls correctly using the servo calibration Arduino sketch. The data transmission from the potentiometers to the Nano through the multiplexer should also be checked by flashing the HEDAS Arduino sketch and using the serial monitor.

Figure 5.4a shows a photo of the glove assembly, which is connected to a portable power bank, which is mounted to the upper arm using a phone arm band. The USB cable for the Nano, as well as the VIVE tracker and mount are not implemented in this photo.

The hardware should be completely built. Finally, the sequence of software that will allow for testing and simulation of the haptic gloves (discussed in Section 6.1) is as follows:

1. Flash the HEDAS sketch to the Nano (if it has not been already flashed during the optional validation step above).

2. Run the sim.py script to start the PyBullet Mano simulation. Finally, run the HEDAS.py script. Follow the instructions as shown on the GUI to complete calibration of the glove.

3. Once calibration is complete, the PyBullet Mano simulation should begin and the user should be able to test the haptic feedback glove in the sample testing environment provided.

Some pointers and tips during assembly:

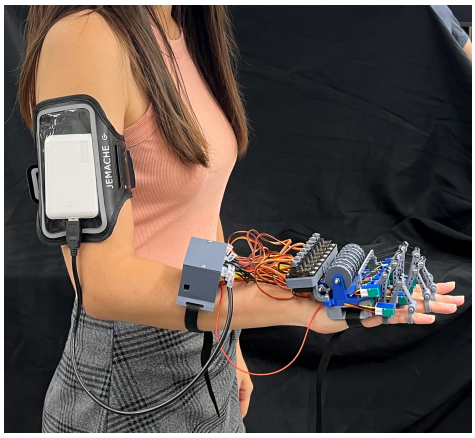

(a) Overview

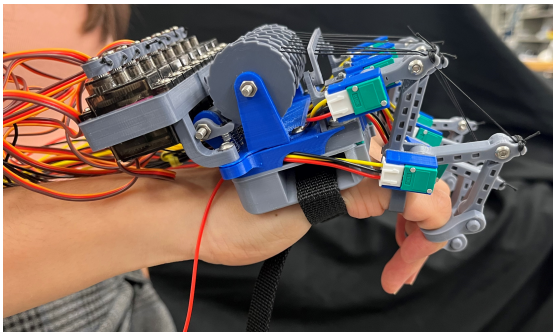

(b) Side View

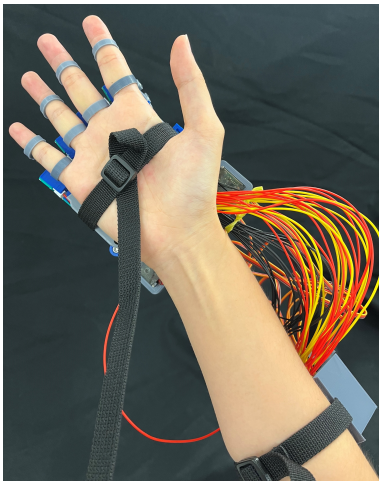

(c) Bottom (Palmar) View

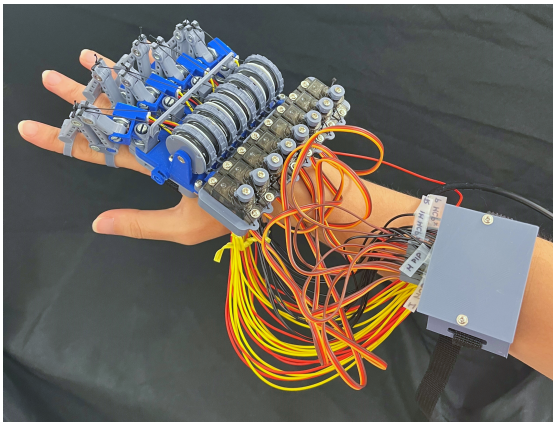

(d) Top (Dorsal) View

Figure 5.4: Glove Assembly

- The ease of assembly/mechanisms used for the haptic feedback mechanism depend heavily on the fit of the 3D printed parts. The assembly process will be more difficult if the M3 hex nuts cannot be held in place by the press fit into the slots. The haptic feedback mechanism will not work if the ratchet gear does not tightly snap fit the badge reel spool; it cannot be allowed to rotate independent of the spool, and must be attached such that the two parts are coaxial. The shaft must be loose fitting through the hole of the ratchet gear; if there is any friction between the two parts, the spool assembly will not spin smoothly.

- It is very helpful to have thorough labelling throughout the assembly process as the number of wires and spools and strings can become overwhelming and confusing. Twist ties are also very helpful in organizing wires.

- It is very difficult to disassemble/re-assemble the long threaded rod with all of the spools on it if one of the spools on the end/middle are not working well. It is much better to test each individual spool assembly by hand or by itself on a separate M3 screw. all of the spools should be assembled on the M3 threaded rod only after each spool assembly has been validated.

- If it is not the friction between the shaft and the ratchet gear that is causing the spool assembly to not turn freely, it is likely the coil spring itself. The end of the strip may be rubbing against the other strips as they close in, so it is important to snip the excess length of spring and have the end curved in a way that secures it to the shaft, but also prevents friction between the sharp end and the rest of the spring.

- When assembling all of the spool assemblies onto the $90mm$ M3 threaded rod, it is best to secure the wound threads with a piece of tape so that each spool assembly can simply be spun down the rod. If the thread is left unsecured, the rotation of turning the spool assembly down the rod will cause the wound thread to unwind, tangle, and become a mess. Do not remove the tape securing the threads until all spool assemblies have been mounted, secured, and the whole rod has been mounted on the haptic feedback mechanism attachments.

Chapter 6

Testing and Validation

6.1 Test Environment and Setup

To validate the design, a VR test environment is required. There are existing open-source environments that provide hand modelling and collision detection, so it is not necessary to develop an environment from scratch. Inspired by simulations ([35], [31]) that utilize a popular open-source physics simulator called Pybullet [21], a package called "mano_pybullet," developed by Kalevatykh [36] is used. Mano_pybullet combines the Pybullet physics simulator with Mano, a hand model developed by Romero et al. [46] that utilizes a kinematic model with the same DOFs as Lee and Kunii's model, so the package is a great match that can be modified to develop a testing environment.

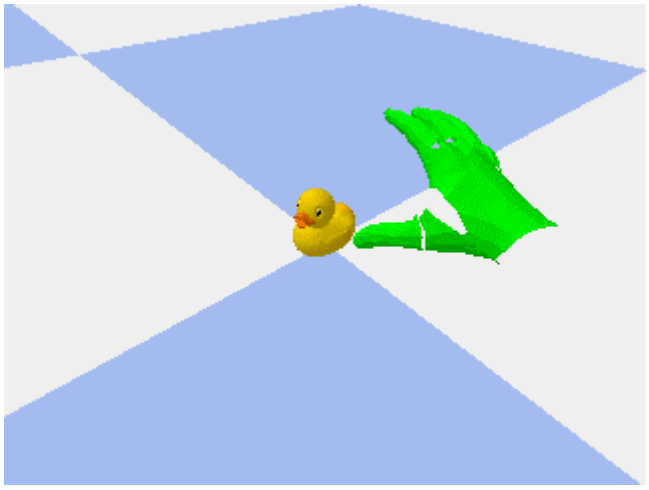

Figure 6.1: Sample Mano Pybullet Simulation Environment [36]

As mentioned in Section 3.2, the original HEDAS python code connects to a socket which forwards joint angle data to an executable after calibration of the glove is complete. For haptic feedback validation, the connection is re-routed to the Mano simulation, where the existing package can model the hand and provide objects that can be interacted with. The environment returns an array of binaries that represents if collision occurred for any of the links in the hand back to the HEDAS python script. The HEDAS script is modified to process the incoming data; the collision array is truncated so that an array containing only the links of interest are forwarded through serial communication to the Nano. The Nano actuates the servo responsible for the corresponding link according to the collision status. If there is no collision, the servo turns to a position that pulls on the pawl string, thus disengaging the pawl from the ratchet gear, to allow unrestricted movement. If collision is present, the servo turns to a position that provides slack in the pawl string, thus allowing the pawl to engage with the ratchet gear and prevent further flexion of the corresponding joint.

To prove that the proximal and intermediate phalanges can receive independent haptic feedback, an environment with a simple cylinder fixed in space is used. Since the cylinder does not come with the mano_pybullet package, the cylinder is added to the environment by creating a URDF file for the desired object. For the sake of simplicity, the VIVE tracker is not used during preliminary testing. Instead, the wrist is also fixed in space such that the fingers hover closely over the cylinder. Additionally, the thumb is not actuated, since it is omitted in the assembly. The haptic feedback is tested with the cylinder fixed in various positions so that the independence of haptic feedback between the proximal and intermediate phalanges can be validated. Users are able to contact the cylinder with either the intermediate or proximal phalanges, or wrap their fingers around the cylinder to contact both phalanges simultaneously.

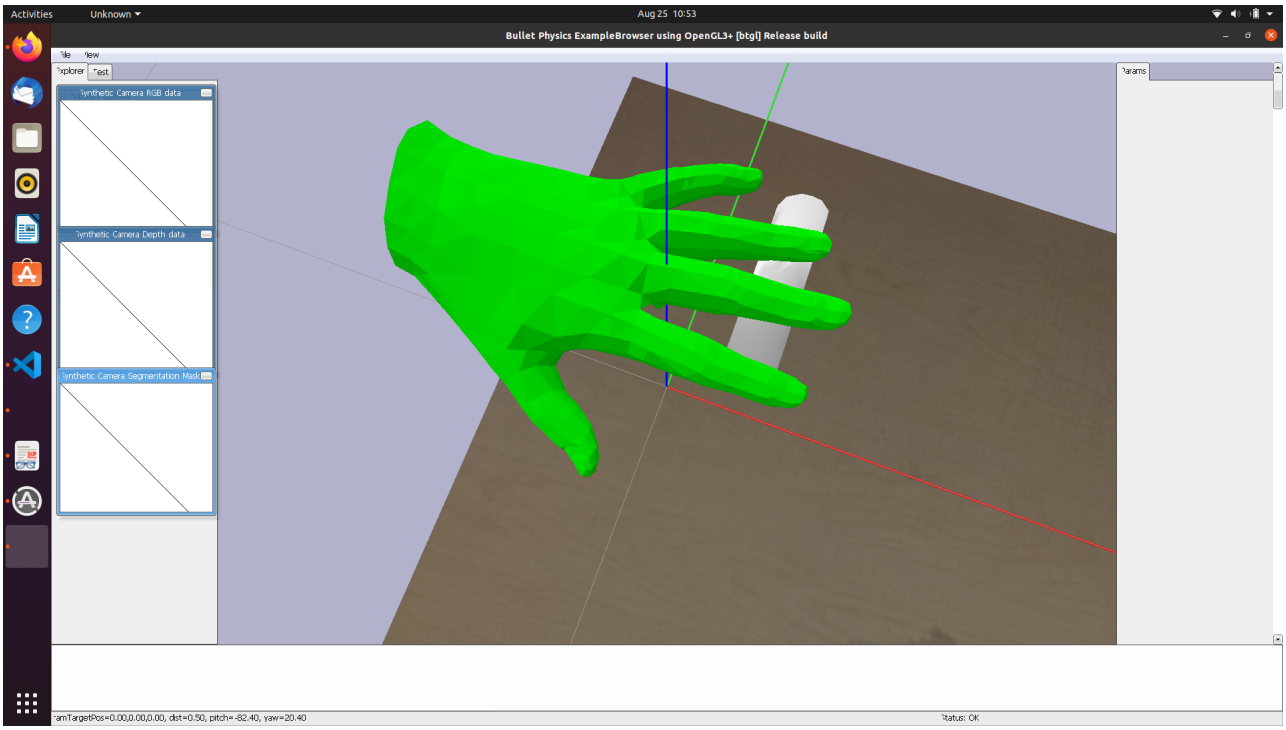

Figure 6.2: Test Setup to Validate Haptic Feedback to the Intermediate Phalanges

6.2 Results

Preliminary testing shows that the haptic mechanism design is successful. Visually, the hand model in the mano_pybullet simulation updates seemingly instantaneously to mirror the hand pose. When the phalanges contact the cylinder, the servos successfully engage and disengage accordingly, applying constraints to the fingers such that further flexion is not possible, but extension is possible. When the cylinder is positioned such that only the proximal phalanges are contacting, the intermediate phalanges can still be flexed or extended, demonstrating independence in haptic feedback of the two regions. However, if the intermediate phalanges are constrained, the proximal phalanges are also constrained, as the linkages for the intermediate phalanges are dependent on the linkages for the respective proximal phalanges. An example scenario in which the intermediate phalanges may be constrained, but not the proximal phalanges or palm, is when a ledge is grasped. If only the

intermediate phalanges are contacted, the palm and proximal phalanges should be able to rotate about the PIP joints. In contrast, when the glove provides haptic feedback, the ratchet and pawl mechanism prevents any increase in distance between the spool and the linkage connected by the string. Therefore, the proximal phalanges and palm are constrained such that they can only rotate in a direction that will decrease the distance between the spool and the intermediate phalanx linkage, not increase. However, this discrepancy is difficult to notice because it is extremely difficult to simulate this scenario; in reality, the ledge acts as a fixed support that resists all translational and rotational forces. The glove can only provide normal force feedback, so when a similar scenario is presented in VR, the entire hand moves when attempting to perform a similar hinging motion.

The time taken for the main loop of the modified Arduino script and the modified HEDAS script to send, modify, and receive data between the Nano and Mano simulation is measured to be $8ms$ total. Therefore, the system performs well below the threshold of $200ms$ and will provide a seamless, seemingly instantaneous user experience. It is possible that additional latency from the Mano simulation could be slow enough that it is noticeable to the user, but the latency for the simulation is dependent on the user's computational power. The processor and GPU that is being used in the main computer are uncontrollable design variables; thus, the response time of the Mano simulation is not considered. Since this is a graphics based simulation, it is recommended that a dedicated GPU is used to minimize the simulation latency.

Chapter 7

Conclusions

7.1 Evaluation Using Design Objectives

The haptic glove design proposed in this thesis meets many of the goals outlined in Section 1.4. The minimum total cost for one glove is within the range deemed reasonable in the market survey by Aujas [16], and is significantly cheaper than commercial haptic gloves. The glove does not require extensive expertise to assemble, though soldering and assembly of the small parts may be a little challenging for consumers with very large hands. The average $8ms$ latency of the system is well below the threshold of $200ms$, and in testing, mirrored the hand pose and provided feedback seemingly instantaneously. Although grounding is minimized, the design relies on a USB cable to communicate via serial protocol to the computer. However, the USB cable does not limit the user's movement significantly, and the range of movement can be adjusted by selecting the length of the USB cable used. The design is compatible with all VR systems, as it does not rely on external systems to determine the pose of the hand. However, depending on the system used, the tracker used to measure the 6 DOFs at the wrist will change. For this thesis, the VIVE tracker is used, and is reflected in the design of the tracker mount. If a different system is used, the tracker mount should be modified accordingly. During testing, the system is able to provide feedback to the areas of interest. The intermediate phalanges are able to flex and extend independently from their respective proximal phalanges, however, when the intermediate phalanges are constrained,

the proximal phalanges become constrained as well.

Although no significant issues with the ergonomics and form of the design were noticed during testing and validation, the system has not been tested by various users, so no definitive conclusions can be made regarding these goals.

7.2 Limitations and Future Work

The current design does not have additional areas for expansion. Ideally, haptic feedback to the fingertips as well as the thumb and palms should be implemented for a more realistic and immersive user experience, but there is no remaining space on the top plate to develop these extensions. Therefore, it is expected that further expansion of haptic feedback using this design will be challenging and may require significant redesign. Alternative mounting arrangements of the spools should be explored to address this issue.

As shown in the actuator selection process, the weight of the design is of secondary priority to the cost. Although the weight is maintained such that it does not impact the usability of the glove, the weight of the glove is not trivial and it is possible that users may experience fatigue or strain with prolonged use. To reduce impact of the weight of the system, the motors should be mounted to the forearm, thus distributing the weight across a larger area of the hand and arm. Additionally, parameters such as the number of gear teeth on the ratchet, which impacts the resolution of the haptic feedback mechanism, are not optimized. These parameters have significant impact to the user experience, so they should be optimized when the design is refined in future work.

The resolution of the system, as well as the amount of time required to 3D print the parts are heavily dependent on the manufacturing abilities, so the capabilities of FDM should be

evaluated to determine optimal print settings that effectively balance the required printing time and accuracy of the printed parts.

As mentioned in Section 3.1, modern power banks often feature auto-off functions that prevent power from being supplied to circuits that draw low currents. A more optimal solution should be researched and implemented in the future.

The current design is manufactured using PLA, a rigid thermoplastic, so the ring diameters of each glove must be tailored to each user. It may be possible to improve the versatility of the glove to accommodate hands of various sizes by printing the finger rings using a more elastic material. Ways to make the design more adaptable for hands of various sizes should be investigated, so that one glove can be used by multiple people.

The ergonomics of the design has not been thoroughly tested, and should be further studied through surveys and testing by various users.

The system should be tested with the implementation of hand position tracking, using either the VIVE tracker discussed in this thesis, or a different tracker of choice. Then, further work may be done to apply the glove to existing VR games, similar to how LucidGloves can be used in existing games through game modifications and interfacing with gaming platforms such as Steam.

Lastly, the current design is not wireless due to the use of serial communication over a USB cable. However, the design can be made completely wireless if the data communication is done over wireless methods such as Bluetooth. The current microcontroller does not have a Bluetooth module, so either a module must be added to the current hardware, or a new microcontroller with Bluetooth functionality can be used. It is unclear how much Bluetooth will impact factors such as the latency of the system. The modification of the current design to be wireless should be explored to improve the portability of the system and minimize

movement restrictions imposed on the user.

Bibliography

[1] Amazon. 12PCS MG90S Servo Micro 180° 9G Servo Motor Geared Micro Servo Motor 9G Smart Robot Compatible with Raspberry Pi Project Car Helicopter Airplane Boat (Control Angle 180), . URL https://www.amazon.com/Dorhea-Helicopter-Airplane-Walking-Compatible/dp/B0925V3X2S/ref=sr_1_7?keywords=mini%2Bservo%2Bmotor&qid=1692582666&sr=8-7&th=1.

[2] Amazon. 12PCS SG90 Micro Servo Motor, Dorhea Mini Servo SG90 9g Servo Kit for RC Helicopter Airplane Car Boat Robot Arm/Hand/Walking/Servo Door Lock Control, . URL https://www.amazon.com/Dorhea-Helicopter-Airplane-Walking-Compatible/dp/B08FJ27Q1H/ref=sr_1_7?keywords=mini%2Bservo%2Bmotor&qid=1692582666&sr=8-7&th=1.

[3] Amazon. Anker PowerCore 5000 Portable Charger, Ultra-Compact 5000mAh External Battery with Fast-Charging Technology, Power Bank for iPhone, iPad, Samsung Galaxy and More, . URL https://www.amazon.com/Anker-PowerCore-Ultra-Compact-High-Speed-Technology/dp/B01CU1EC6Y/ref=pd_bxgy_sccl_1/137-6745375-1135228?pd_rd_w=BZxys&content-id=amzn1.sym.26a5c67f-1a30-486b-bb90-b523ad38d5a0&pf_rd_p=26a5c67f-1a30-486b-bb90-b523ad38d5a0&pf_rd_r=J7AYZ1TKTYBKVGRBZYD6&pd_rd_wg=y3ZQY&pd_rd_r=38be90fa-cfbc-4e4e-a899-f66b1f53b8fd&pd_rd_i=B01CU1EC6Y&psc=1.

[4] Amazon. Anker Portable Charger with Built-in Lightning Connector, MFi Certified, Battery Pack 5,000mAh 12W, Compatible with iPhone 14/14

Pro / 14 Plus / 14 Pro Max, iPhone 13 and 12 Series (Black), . URL https://www.amazon.com/Anker-Lightning-Connector-Certified-Compatible/dp/B0BV5YV836?ref_=ast_sto_dp&th=1.

[5] Amazon. Anker 321 Power Bank (PowerCore 5K), 5,200mAh Portable Charger, Compatible with iPhone 13 and 12 Series, Samsung, Google Pixel, LG, and More, . URL https://www.amazon.com/Anker-PowerCore-Ultra-Compact-Portable-Compatible/dp/B09NRG2YT3/?tag=maketecheas08-20&th=1.

[6] Amazon. Charmast Portable Charger, Smallest 10000 Quick Charge Battery Pack, USB C Power Bank Fast Charging Mini Portable Battery Charger for iPhone, Samsung, Pixel, LG, TCL, OnePlus, Motorola, More Phones, . URL https://www.amazon.com/Charmast-Smallest-Portable-10400mah-Compatible/dp/B07L931FCY/ref=sr_1_4?keywords=smallest%2Bpower%2Bbank&qid=1688719030&sr=8-4&th=1.

[7] Amazon. FLASH HOBBY 2PCS FH-2502 Nano Servo 2g Steering Gear with JST 1.25 Interface for RC Micro Indoor Aircraft Airplane Engine Spare Parts (JST1.25), . URL https://www.amazon.com/FLASH-HOBBY-Steering-Interface-Aircraft/dp/B08NPHG99D/ref=sr_1_27?keywords=micro%2Bservo&qid=1692589868&s=toys-and-games&sr=1-27&th=1.

[8] Amazon. FOCHEW Portable Charger, 2-Pack 20000mAh Power Bank Ultra Slim Fast Charging External Battery Pack with Dual USB Outputs Compatible with iPhone 13/12 Pro/12/11/XR/X, Samsung S20, Tablet etc., . URL https://www.amazon.com/dp/B094G1GL8T/ref=cm_sw_r_cp_api_glt_fabc_DW1G0CYTDMAXEMEMPS3Y?_encoding=UTF8&th=1.

[9] Amazon. INIU Portable Charger, Slimmest 10000mAh 5V/3A Power Bank, USB

C in&out High-Speed Charging Battery Pack, External Phone Powerbank Compatible with iPhone 14 13 12 11 Samsung S22 S21 Google LG iPad etc, . URL https://www.amazon.com/dp/B07CZDXDG8?tag=rollingston07-20&linkCode=ogi&th=1&language=en_US&asc_source=amp&asc_campaign=amp&asc_refurl=https%3A%2F%2Fwww.rollingstone.com%2Fproduct-recommendations%2Felectronics%2Fbest-small-power-banks-portable-chargers-985561%2F.

[10] Amazon. INIU Portable Charger, Small 10000mAh Power Bank USB C In/Output 22.5W Fast Charging, 3-Output Mini Battery Pack Charger with Phone Holder for iPhone 14 13 12 11 Pro Samsung S23 A53 Google iPad Tablet, . URL https://www.amazon.com/INIU-Portable-Charging-10000mAh-Tablets/dp/B09176JCKZ/ref=sr_1_3_mod_primary_new?keywords=mini%2Bpower%2Bbanks&qid=1688712822&s=wireless&sbo=RZvfv%2F%2FHxDF%2BO5021pAnSA%3D%3D&sr=1-3&th=1.

[11] Amazon. Miady 2-Pack 5000mAh Mini Portable Charger, Power Pack with 5V 2.4A USB Output, Power Bank Phone Charger for iPhone XR, 11, 12, Android Phones and etc, . URL https://www.amazon.com/Miady-5000mAh-Portable-Charger-Android/dp/B08T8TDS8S/ref=sr_1_3?keywords=mini%2Bpower%2Bbank&qid=1688720688&sr=8-3&th=1.

[12] Amazon. RCmall 4Pcs DM-S0020 2.1g Ultra-Micro Servo Coreless Motor 2g Digital Servo with JR Connector 3.7V-5V for RC Hobby, . URL https://www.amazon.com/RCmall-DM-S0020-Ultra-Micro-Coreless-Connector/dp/B0B6PNPDN4/ref=sr_1_20?keywords=micro+servo&qid=1692589868&s=toys-and-games&sr=1-20.

[13] Amazon. YoungRC Micro 3.7g Servo GH-S37D Mini Digital Servo for Control Aeromodelling Aircraft Flight Direction RC Plane Helicopter Boat Car 5pcs, . URL https://www.amazon.com/YoungRC-Aeromodelling-Aircraft-Direction-Helicopter/

dp/B082SM99HL/ref=sr_1_21?keywords=micro+servo&qid=1692586800&s=toys-and-games&sr=1-21.

[14] Jinung An and Dong-soo Kwon. Haptic experimentation on a hybrid active/passive force feedback device. In *Proceedings 2002 IEEE International Conference on Robotics and Automation (Cat. No.02CH37292)*, volume 4, pages 4217–4222 vol.4, May 2002. doi: 10.1109/ROBOT.2002.1014416.

[15] Arduino. Arduino Nano. URL https://store-usa.arduino.cc/products/arduino-nano.

[16] Thomas Aujas. *Development of a low cost and easy to assemble glove for hand movement acquisition as an open- source project*. PhD thesis, Staffordshire University, August 2021.

[17] Ismail Ben Abdallah, Yassine Bouteraa, and Chokri Rekik. Design and development of 3d printed myoelectric robotic exoskeleton for hand rehabilitation. *International Journal on Smart Sensing and Intelligent Systems*, 10:341–366, June 2017. doi: 10.21307/ijssis-2017-215.

[18] Ian M. Bullock, Júlia Borràs, and Aaron M. Dollar. Assessing assumptions in kinematic hand models: A review. In *2012 4th IEEE RAS & EMBS International Conference on Biomedical Robotics and Biomechatronics (BioRob)*, pages 139–146, June 2012. doi: 10.1109/BioRob.2012.6290879. ISSN: 2155-1782.

[19] Manuel Caeiro-Rodríguez, Iván Otero-González, Fernando A. Mikic-Fonte, and Martín Llamas-Nistal. A Systematic Review of Commercial Smart Gloves: Current Status and Applications. *Sensors*, 21(8):2667, April 2021. ISSN 1424-8220. doi: 10.3390/s21082667. URL https://www.mdpi.com/1424-8220/21/8/2667.

[20] Daniel Cooper. You can now buy the software behind Imogen Heap's

musical gloves, February 2021. URL https://www.engadget.com/glover-mi-mu-gloves-standalone-software-audio-gestures-sound-130004470.html.

[21] Erwin Coumans and Yunfei Bai. Pybullet, a python module for physics simulation for games, robotics and machine learning. http://pybullet.org, 2016–2021.

[22] Creality. Ender-3 Pro 3D Printer. URL https://www.creality.com/products/ender-3-pro-3d-printer.

[23] Lucas De Bonet. LucidGloves: VR Haptic Gloves on a budget, March 2021. URL https://hackaday.io/project/178243-lucidgloves-vr-haptic-gloves-on-a-budget.

[24] Lucas De Bonet. LucidGloves - Firmware and 3D Printer Files, August 2023. URL https://github.com/LucidVR/lucidgloves. original-date: 2021-04-20T03:01:47Z.

[25] Ashish D. Deshpande, Zhe Xu, Michael J. Vande Weghe, Benjamin H. Brown, Jonathan Ko, Lillian Y. Chang, David D. Wilkinson, Sean M. Bidic, and Yoky Matsuoka. Mechanisms of the Anatomically Correct Testbed Hand. *IEEE/ASME Transactions on Mechatronics*, 18(1):238–250, February 2013. ISSN 1083-4435, 1941-014X. doi: 10.1109/TMECH.2011.2166801. URL http://ieeexplore.ieee.org/document/6032103/.

[26] Mihai Dragusanu, Alberto Villani, Domenico Prattichizzo, and Monica Malvezzi. Design of a Wearable Haptic Device for Hand Palm Cutaneous Feedback. *Frontiers in Robotics and AI*, 8:706627, September 2021. ISSN 2296-9144. doi: 10.3389/frobt.2021.706627. URL https://www.frontiersin.org/articles/10.3389/frobt.2021.706627/full.

[27] EIDBadges. Badge Reel Anatomy. URL https://www.eidbadges.com/anatomy-reels.

[28] Evan-Amos. English: The front and back of a human right hand., April 2012. URL https://commons.wikimedia.org/wiki/File:Human-Hands-Front-Back.jpg.

[29] Thomas Feix, Javier Romero, Heinz-Bodo Schmiedmayer, Aaron M. Dollar, and Danica Kragic. The GRASP Taxonomy of Human Grasp Types. *IEEE Transactions on Human-Machine Systems*, 46(1):66–77, February 2016. ISSN 2168-2305. doi: 10.1109/THMS.2015.2470657. Conference Name: IEEE Transactions on Human-Machine Systems.

[30] Jamie Feltham. bHaptics Reveals TactGlove $299 Haptic VR Gloves For Quest 2, December 2021. URL https://uploadvr.com/tactsuit-vr-gloves-bhaptics-announced/. Section: VR Hardware.

[31] Soheil Habibian, Ananth Jonnavittula, and Dylan P. Losey. *Here's What I've Learned:* Asking Questions that Reveal Reward Learning. *ACM Transactions on Human-Robot Interaction*, 11(4):1–28, December 2022. ISSN 2573-9522, 2573-9522. doi: 10.1145/3526107. URL https://dl.acm.org/doi/10.1145/3526107.

[32] Haptx. Haptic Gloves G1 - Gloves for virtual reality and robotics | HaptX Pre-Order. URL https://g1.haptx.com/.

[33] Christopher-Eyk Hrabia, Katrin Wolf, and Mathias Wilhelm. Whole hand modeling using 8 wearable sensors: biomechanics for hand pose prediction. In *Proceedings of the 4th Augmented Human International Conference*, pages 21–28, Stuttgart Germany, March 2013. ACM. ISBN 978-1-4503-1904-1. doi: 10.1145/2459236.2459241. URL https://dl.acm.org/doi/10.1145/2459236.2459241.

[34] Ya Huang, Kuanming Yao, Jiyu Li, Dengfeng Li, Huiling Jia, Yiming Liu, Chun Ki Yiu, Wooyoung Park, and Xinge Yu. Recent advances in multi-mode haptic feedback technologies towards wearable interfaces. *Materials Today Physics*, 22:100602, January

2022. ISSN 25425293. doi: 10.1016/j.mtphys.2021.100602. URL https://linkinghub.elsevier.com/retrieve/pii/S2542529321002637.

[35] Ananth Jonnavittula and Dylan P. Losey. I Know What You Meant: Learning Human Objectives by (Under)estimating Their Choice Set, April 2021. URL http://arxiv.org/abs/2011.06118. arXiv:2011.06118 [cs].

[36] Igor et al. Kalevatykh. mano_pybullet - porting the mano hand model to the pybullet simulator. Github, 2020. URL https://github.com/ikalevatykh/mano_pybullet.

[37] Jintae Lee and T.L. Kunii. Model-based analysis of hand posture. *IEEE Computer Graphics and Applications*, 15(5):77–86, September 1995. ISSN 1558-1756. doi: 10.1109/38.403831. Conference Name: IEEE Computer Graphics and Applications.

[38] Mi.Mu Gloves Limited. MiMU Gloves. URL https://mimugloves.com/gloves/.

[39] Bor-Shing Lin, I.-Jung Lee, Shu-Yu Yang, Yi-Chiang Lo, Junghsi Lee, and Jean-Lon Chen. Design of an Inertial-Sensor-Based Data Glove for Hand Function Evaluation. *Sensors*, 18(5):1545, May 2018. ISSN 1424-8220. doi: 10.3390/s18051545. URL https://www.mdpi.com/1424-8220/18/5/1545. Number: 5 Publisher: Multidisciplinary Digital Publishing Institute.

[40] Laszlo Lipot. Mechanisms: Ratchet and Pawl. URL https://www.notesandsketches.co.uk/Ratchet.html.

[41] Robert B. Miller. Response time in man-computer conversational transactions. In *Proceedings of the December 9-11, 1968, fall joint computer conference, part I on - AFIPS '68 (Fall, part I)*, page 267, San Francisco, California, 1968. ACM Press. doi: 10.1145/1476589.1476628. URL http://portal.acm.org/citation.cfm?doid=1476589.1476628.

[42] Gordon Ng. Flex Sensor Glove. URL https://phys420.phas.ubc.ca/p420_2020/ngg/.

[43] ProtoSupplies. Servo Motor Micro MG90S. URL https://protosupplies.com/product/servo-motor-micro-mg90s/.

[44] Shadow Robot. Shadow Hand & Glove for Dexterous Manipulation, September 2022. URL https://www.shadowrobot.com/shadow-hand-glove/.

[45] Rokoko. Rokoko Store - Buy the Smartgloves, the best finger tracking gloves on the market. URL https://us.store.rokoko.com/products/smartgloves.

[46] Javier Romero, Dimitrios Tzionas, and Michael J. Black. Embodied hands: Modeling and capturing hands and bodies together. *ACM Transactions on Graphics, (Proc. SIGGRAPH Asia)*, 36(6), November 2017.

[47] Internal Revenue Service. Yearly Average Currency Exchange Rates | Internal Revenue Service, February 2023. URL https://www.irs.gov/individuals/international-taxpayers/yearly-average-currency-exchange-rates.

[48] Bukun Son and Jaeyoung Park. Haptic Feedback to the Palm and Fingers for Improved Tactile Perception of Large Objects. October 2018. doi: 10.1145/3242587.3242656.

[49] TESLASUIT. Haptic Glove for Virtual Reality with Force Feedback | TESLAGLOVE. URL https://teslasuit.io/products/teslaglove/.

[50] Exchange Rates UK. British Pound to US Dollar Spot Exchange Rates for 2021. URL https://www.exchangerates.org.uk/GBP-USD-spot-exchange-rates-history-2021.html.

[51] Ultraleap. Leap motion controller 2 – Ultraleap. URL https://leap2.ultraleap.com/leap-motion-controller-2/.

[52] HTC VIVE. VIVE Tracker (3.0) | VIVE United States. URL https://www.vive.com/us/accessory/tracker3/.

[53] Lefan Wang, T. Meydan, and Paul Williams. A Two-Axis Goniometric Sensor for Tracking Finger Motion. *Sensors*, 17, April 2017. doi: 10.3390/s17040770.